

Review

An Overview of Technological Parameter Optimization in the Case of Laser Cladding

Kaiming Wang^{1,2,3,4} , Wei Liu¹, Yuxiang Hong² , H. M. Shakhawat Sohan¹, Yonggang Tong^{1,*} , Yongle Hu¹ , Mingjun Zhang¹, Jian Zhang¹, Dingding Xiang^{3,4}, Hanguang Fu⁵  and Jiang Ju^{6,*} 

¹ College of Automotive and Mechanical Engineering, Changsha University of Science and Technology, Changsha 410114, China

² Key Laboratory of Intelligent Manufacturing Quality Big Data Tracing and Analysis of Zhejiang Province, China Jiliang University, Hangzhou 310018, China

³ State Key Laboratory of Tribology in Advanced Equipment, Department of Mechanical Engineering, Tsinghua University, Beijing 100084, China

⁴ Key Laboratory of Vibration and Control of Aero-Propulsion Systems, Ministry of Education, Northeastern University, Shenyang 110819, China

⁵ Key Laboratory of Advanced Functional Materials, Ministry of Education, Department of Materials Science and Engineering, Beijing University of Technology, Beijing 100124, China

⁶ Department of Materials Science and Engineering, City University of Hong Kong, Hong Kong 999077, China

* Correspondence: yg_tong@csust.edu.cn (Y.T.); jiang.ju@cityu.edu.hk (J.J.)

Abstract: This review examines the methods used to optimize the process parameters of laser cladding, including traditional optimization algorithms such as single-factor, regression analysis, response surface, and Taguchi, as well as intelligent system optimization algorithms such as neural network models, genetic algorithms, support vector machines, the new non-dominance ranking genetic algorithm II, and particle swarm algorithms. The advantages and disadvantages of various laser cladding process optimization methods are analyzed and summarized. Finally, the development trend of optimization methods in the field of laser cladding is summarized and predicted. It is believed that the result would serve as a foundation for future studies on the preparation of high-quality laser cladding coatings.

Keywords: laser cladding; process parameter; optimization methods; review



Citation: Wang, K.; Liu, W.; Hong, Y.; Sohan, H.M.S.; Tong, Y.; Hu, Y.; Zhang, M.; Zhang, J.; Xiang, D.; Fu, H.; et al. An Overview of Technological Parameter Optimization in the Case of Laser Cladding. *Coatings* **2023**, *13*, 496. <https://doi.org/10.3390/coatings13030496>

Academic Editor: Rafael Comesaña

Received: 1 February 2023

Revised: 16 February 2023

Accepted: 22 February 2023

Published: 23 February 2023



Copyright: © 2023 by the authors. Licensee MDPI, Basel, Switzerland. This article is an open access article distributed under the terms and conditions of the Creative Commons Attribution (CC BY) license (<https://creativecommons.org/licenses/by/4.0/>).

1. Introduction

Laser cladding is a technique for the deposition of a protective layer on a substrate [1,2]. It is the process of depositing a material called a “cladding material” onto a substrate with the help of the thermal energy provided by a laser beam [3–5]. The cladding material could be applied to the substrate by wire feeding, powder injection, or a preset powder [6–8]. Among them, the wire feeding system is very suitable for processing with high deposition rates [9]. However, most cladding materials still use powder because the powder-feeding method is more flexible than wire feeding [10–12]. Laser cladding is an advanced material processing technology in many parts of the business world [13–15]—for example, the metallurgical industry, mining machinery industry, marine industry, aerospace industry, automotive industry, and biomedical industry [16–21]. The laser cladding aims to increase the substrate’s hardness, wear resistance, corrosion resistance, and oxidation resistance [22–26]. It offers significant advantages over conventional surface modification techniques, such as smaller heat-affected zones, lower dilution, good metallurgical bonding with the substrate, and a finer grain size [27–31]. However, the process parameters in the cladding process have an important influence on the quality of the laser cladding coating. If the process parameters are not appropriate, the coating will have defects such as holes and cracks. Therefore, the process parameters must be effectively controlled to obtain the desired performance [32–34].

The laser cladding process is affected by many factors [35–37]. Among them, the process parameter is one of the critical factors affecting the formation and quality of the cladding layer [38–40]. The cladding process is complex and non-linear due to laser cladding involving more than 19 process parameters [41,42]. Laser power, scanning speed, and powder feeding rate have the most significant influence on the quality of the cladding layer [43]. These three parameters offer the broadest potential window in terms of changing and improving the quality of the cladding layer [44]. Experimental and theoretical studies have shown that the proper selection of input process parameters can significantly improve the properties of the cladding layer [45–47]. To obtain high-quality coatings, many scholars have studied and improved the optimization methods of laser cladding process parameters [48,49]. One approach is to investigate the effect of process parameters on the properties of the cladding layer using empirical–statistical and analytical models, such as the response surface method, linear regression method, and Taguchi method [50], to find the optimal process parameters. Another method is to use intelligent algorithms such as machine learning and metaheuristics to establish a predictive model of the mapping relationship between process parameters and the cladding layer, to achieve the optimization of the process parameters [51,52].

This paper reviews the current research status on the optimization of process parameters in laser cladding. It summarizes the optimization methods of various process parameters from traditional and intelligence optimization methods. Then, the advantages and disadvantages of various optimization methods are contrasted. Finally, we provide an outlook on the development trend of optimization methods for the laser cladding process. We hope to provide a reference for future research on the manufacturing of high-quality laser cladding coatings.

2. Traditional Optimization Methods

2.1. Single-Factor Experiment

The traditional single-factor experiment is the most common way to characterize the influence of each parameter on the coating properties [53]. Controlling a single parameter to obtain the desired property is more accessible than controlling multiple parameters [54].

In the study of laser cladding process parameters, many scholars have adopted single-factor experiments to study the process parameters in which they are interested. Among them, the more studied parameters are the laser power, powder feeding rate, and scanning speed [55–58]. Pornsak et al. [59] observed the cladding process in real time by using an infrared camera with image analysis software. The results showed that the laser spot, melt pool area, cladding height, and width all increased with increasing laser power. Zhan et al. [60] found that as the laser power increased, the clad height, width, and grain size also increased. Li [61] and Jiao et al. [62] found that the microhardness of the coating increased as the scanning speed increased. However, the wear properties of the coating will deteriorate sharply when the scanning speed is too large. Bartkowski et al. [63] prepared Stellite-6/WC metal-based composite coatings using different laser powers and powder feeding rates. Studies have found that an increase in laser power and powder feeding rate increases the coating thickness. The effects of the laser power, powder feeding rate, and scanning speed on cladding results are shown in Figure 1.

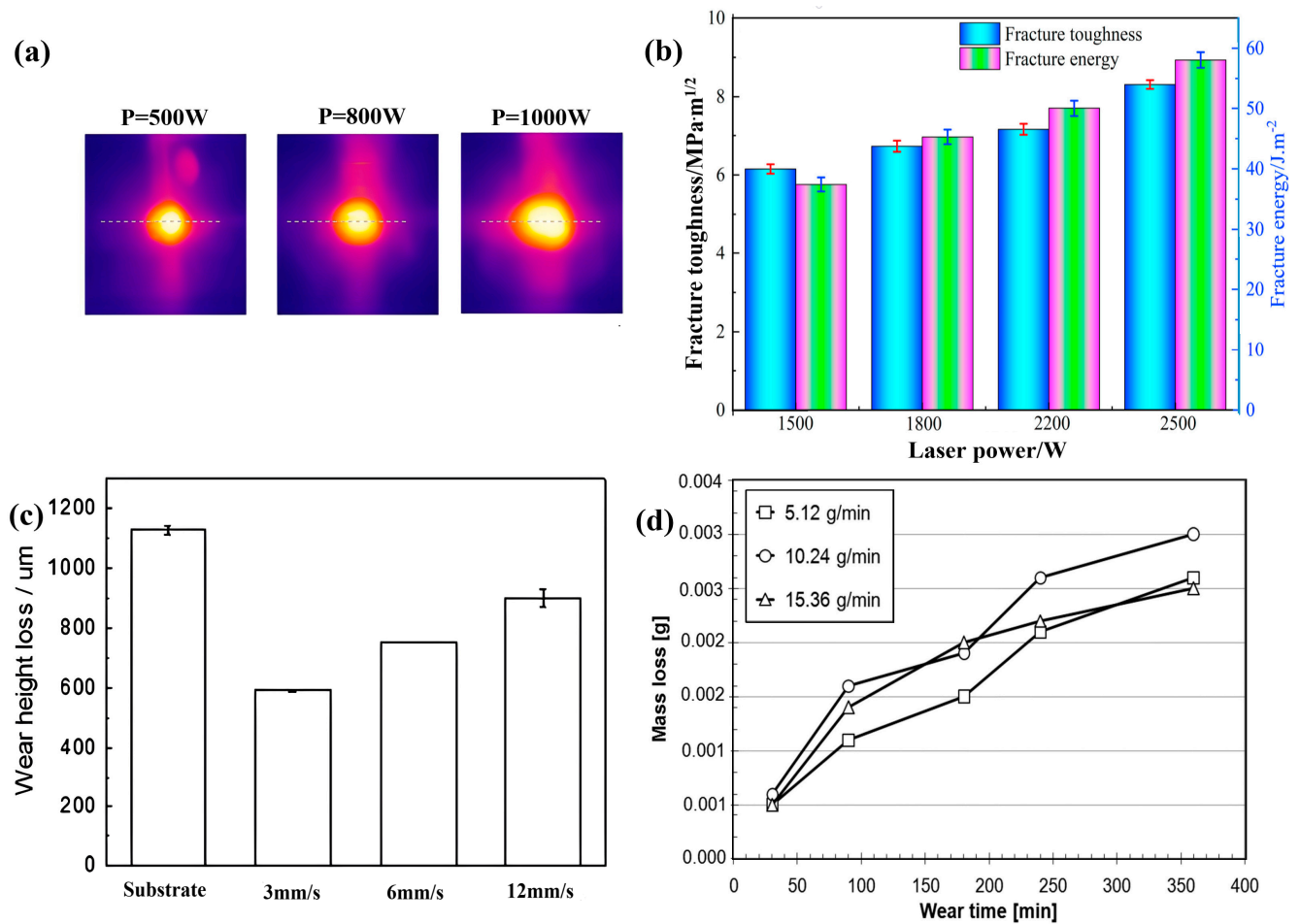


Figure 1. The influence of different laser power, scanning speed, and powder feeding rate on cladding results. (a) Effect of different laser powers on the melt pool. Reprinted from [59]. (b) Fracture toughness and fracture energy of coatings at different laser powers. Reprinted with permission from Ref. [60]. 2022, Elsevier. (c) Wear height losses of substrate and clad layers with different scanning speeds. Reprinted with permission from Ref. [61]. 2013, Taylor and Francis. (d) Effect of different powder feeding rates on the wear resistance of coatings. Reprinted with permission from Ref. [63]. 2016, Elsevier.

Some scholars have studied parameters such as the gas supply speed, laser beam diameter, and pre-placed powder layer thickness. Qi et al. [64] found that the clad width, depth, and height decreased with the increase in the laser beam diameter. Chrystolouris et al. [65] found that the clad depth decreased when increasing the gas supply. Qu et al. [66] analyzed the effects of different pre-coating thicknesses on the cladding layer's microstructure evolution and mechanical properties. They found that the dilution rate of the coating decreased with the increase in the pre-placed powder layer thickness, and the average values of microhardness and fracture toughness increased with the thickness of the pre-coating. The influence of the gas supply speed, laser beam diameter, and pre-coating thickness on the cladding layer is shown in Figure 2.

Above all, a single-factor experiment is a trial-and-error approach. This method often requires extensive experimentation, which is costly and time-consuming. Moreover, since this method studies the effects of only one factor at a time, interactions between input parameters may be overlooked, so the results may not be optimal.

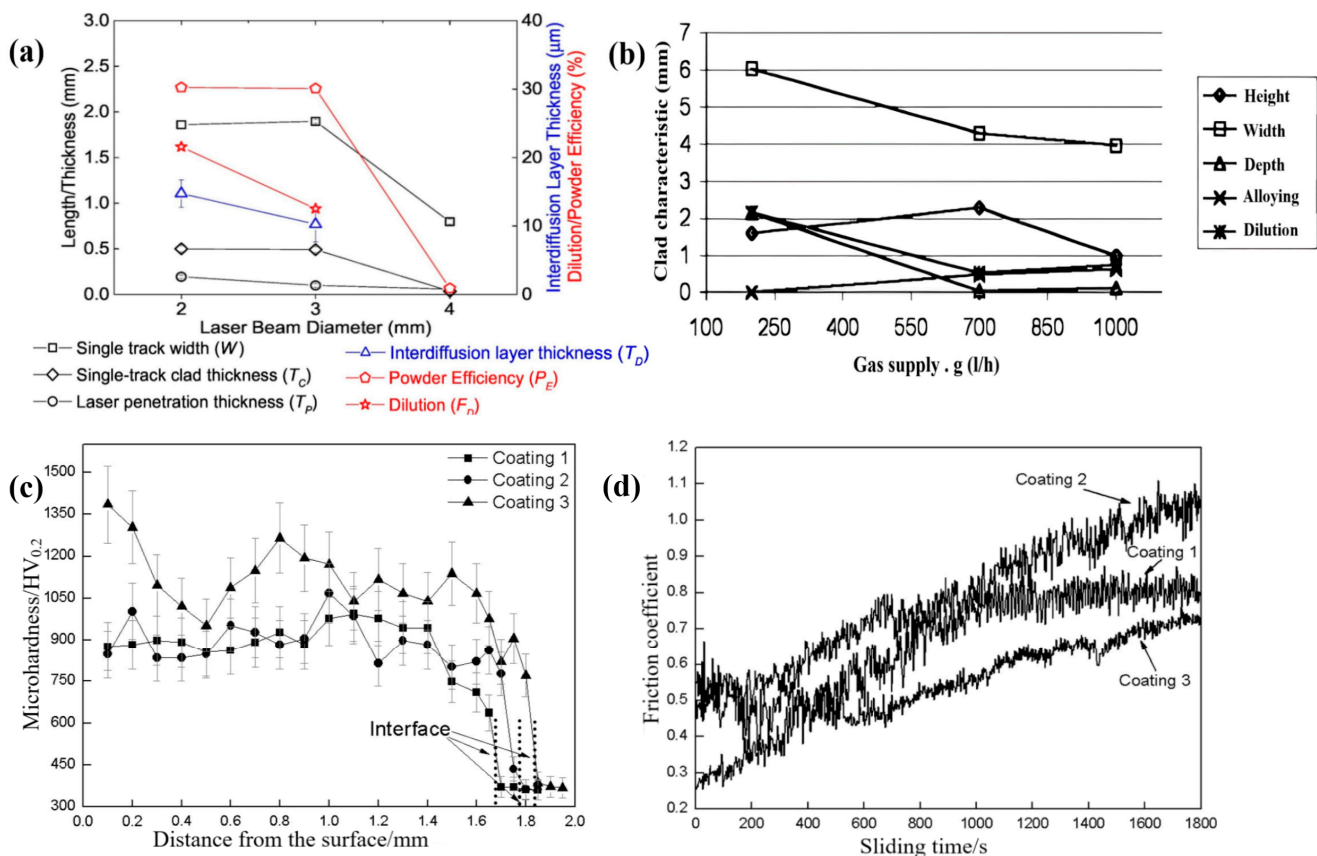


Figure 2. Influence of different laser beam diameters, gas supply speeds, and pre-coating thicknesses on cladding results. (a) Effect of different laser beam diameters on cladding results. Reprinted with permission from Ref. [64]. 2017, Elsevier. (b) The influence of different gas supply speeds on cladding results. Reprinted with permission from Ref. [65]. 2002, Elsevier. (c) Microhardness distribution along the depth direction of the coating under different pre-placed powder layer thicknesses. Reprinted with permission from Ref. [66]. 2015, Elsevier. (d) Variation in coating friction coefficient with sliding time for different pre-placed powder layer thicknesses. Reprinted with permission from Ref. [66]. 2015, Elsevier.

2.2. Regression Analysis

Regression analysis is mainly used to reveal the causal relationship between variables [67] and has been widely used in various types of statistical analysis [68]. It is primarily used as an analysis method in laser cladding to determine the relationship between the process parameters and coating properties. It is widely used in the empirical–statistical model [69,70]. Ansari [71], Shayanfar [72], Erfanmanesh [73], and Nabhani et al. [74] used regression analysis to correlate the main processing parameters (laser power (P), scanning rate (V), powder feeding rate (F)) with the coating's geometrical characteristics (clad height, clad width, penetration depth, wetting angle, and dilution). Afterwards, the relationship between them was investigated using a combined parameter ($P^\alpha V^\beta F^\gamma$). Through this method, they obtained a laser cladding process drawing, from which the best process parameters could be obtained. Through experimental analysis, they discovered that the laser power influences the clad height and the clad width by the combined parameters of the laser power and scanning speed, and the clad depth through the combined parameters of the laser power, scanning speed, and powder feeding rate. However, they have different views on the dilution ratio. Since the laser power factor is present in the numerator and denominator of the dilution rate equation, Ansari [71] and Nabhani et al. [74] argue that its effect can be eliminated by simplifying the fraction, while Shayanfar [72] and Erfanmanesh et al. [73] do not adopt this approach. Ansari [71] and Nabhani et al. [74] believe that the

dilution ratio is related to the scanning speed and powder feeding rate. Shayanfar [72] and Erfanmanesh et al. [73] believe that the dilution ratio is related to the combination of the scanning speed, powder feeding rate, and laser power. The combination of process parameters that affect the cladding result is shown in Table 1. The processing diagram of laser cladding is demonstrated in Figure 3.

Table 1. A combination of process parameters that have an impact on cladding results.

Authors [Year/Reference]	Substrate	Cladding Material	Clad Height	Clad Width	Clad Depth	Dilution Ratio
Ansari 2016 [71]	Inconel 738 superalloy	NiCrAlY powder	$P^2V^{-3/2}F$	$P^{3/2}V^{-1/3}$	$PV^{2/3}F^{-2/3}$	VF^{-1}
Shayanfar 2020 [72]	ASTM A592 steel	625 powder	$P^{1/2}V^{-2}F^2$	$P^{1/2}V^{-1/5}$	$P^3V^{-1/2}F^{3/4}$	$P^{1/2}V^2F^{-3/4}$
Erfanmanesh 2017 [73]	AISI 321 steel	WC-12Co powder	$P^2V^{-2}F^{1/4}$	$PV^{-1/2}$	$P^2V^{1/4}F^{-1/4}$	$P^{1/2}V^2F^{-1}$
Nabhani 2017 [74]	Ti-6Al-4V	Ti-6Al-4V powder	$PV^{-1}F^{1/4}$	$PV^{-1/3}$	$PVF^{-1/8}$	$VF^{-1/2}$

P is laser power, V is scanning speed, and F is powder feeding rate.

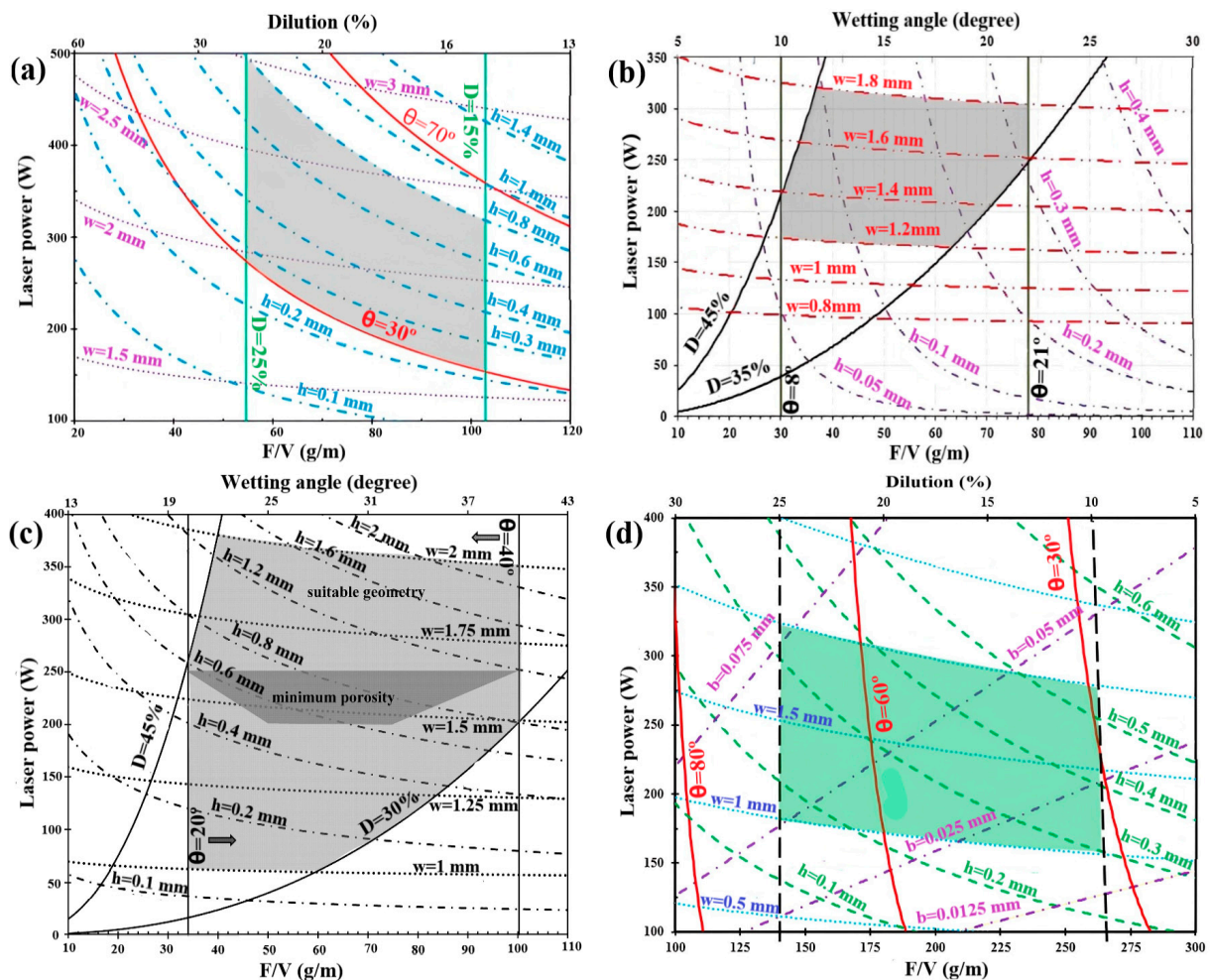


Figure 3. Processing map of laser cladding. (a) The processing map for coaxial laser cladding of NiCrAlY powder on Inconel 738 nickel-based alloys. Reprinted with permission from Ref. [71]. 2016, Elsevier. (b) The processing map for laser cladding of Inconel 625 powder on ASTM A592 steel. Reprinted with permission from Ref. [72]. 2020, Elsevier. (c) The processing map for laser cladding of WC-12Co powder on AISI 321 steel. Reprinted with permission from Ref. [73]. 2017, Elsevier. (d) The processing map for laser cladding of Ti-6Al-4V alloy on Ti-6Al-4V. Reprinted with permission from Ref. [74]. 2018, Elsevier.

Regression analysis can accurately measure the degree of correlation between each factor and the degree of the regression fit to improve the effectiveness of the prediction equation. However, the calculation is more complex. Moreover, for non-linear data or data with complex polynomials, there are difficulties in modeling using the regression analysis method.

2.3. Response Surface Methodology

The response surface methodology is a statistical method that integrates experimental design and mathematical modeling to solve multivariate problems [75,76]. It can be used to improve the secondary effects and interaction effects in different variables [77]. It is an essential branch of experimental design methods that can be used to develop, improve, and optimize processes [78].

In laser cladding, the response surface methodology is a powerful tool in analyzing the relationship between process parameters and cladding results, especially when the response target is affected by multiple process parameters [79,80]. Among them, the three process parameters of laser power, scanning speed, and powder feeding rate are more studied [81]. Cui et al. [82] used the response surface methodology to optimize a cobalt-based alloy coating's process parameters. Their work laid the foundation for the setup of the laser cladding processing parameters for multi-track coatings made from cobalt. The response surface methodology was used by Li et al. [83] to produce a Ni60PTA coating with good properties. The coating did not have any cracks, dents, or holes. Wu et al. [84] studied the relationship between pore formation and multiple process parameters in Ni60A alloy coatings. They found that the powder feeding rate is the main factor affecting the porosity of the coating. The results showed the good surface forming quality of the specimens processed with the optimized process parameters.

Some researchers used the response surface methodology to optimize the laser frequency, pulse width, gas flow, overlap rate, and spot diameter. Khorram et al. [85] found that the laser frequency and pulse width positively affect the clad width, angle, and dilution ratio but negatively affect the clad height and hardness. Lian et al. [86] found that the clad width was inversely proportional to the overlap rate; the dilution ratio was inversely proportional to the gas flow. Within a specific range, the flatness ratio decreases with the increase in gas flow and overlap rate and then increases. Wu et al. [87] prepared a Ni60A-25% laser cladding layer with high microhardness on 42CrMo alloy structural steel. The experimental results show that the effect of the spot diameter on the dilution ratio and effective unit area is minimal. The optimization variables and response indexes used in the response surface methodology are shown in Table 2.

Table 2. Optimization variables and response indexes used in the response surface methodology.

Authors [Year/Reference]	Substrate	Cladding Material	Response Indexes	Optimization Variables	Optimal Process Parameters
Lujun Cui 2021 [82]	ZG310-570 (ZG45)	Co-Cr-W alloy powder	Aspect ratio, dilution rate, clad width, clad height, clad depth	Laser power	1400 W~1700 W
				Powder feeding rate	15 g/min~20 g/min
				Scanning speed	5 mm/s~6 mm/s
Tiankai Li 2022 [83]	45 steel	Ni60PTA alloy powder	Dilution rate, ratio of layer width to height, contact angle	Laser power	1477 W
				Powder feeding rate	17.5 mg/s
				Scanning speed	5 mm/s

Table 2. Cont.

Authors [Year/Reference]	Substrate	Cladding Material	Response Indexes	Optimization Variables	Optimal Process Parameters
Zupeng Wu 2019 [84]	45 steel	Ni60A alloy powder	Porosity area	Laser power	1524.8 W
				Powder feeding rate	5.20 g/min
				Scanning speed	6.72 mm/s
Ali Khorram 2019 [85]	Inconel 718 superalloy	75Cr3C2 + 25(80Ni20Cr) powder	Clad width, clad height, clad angle	Laser frequency	20 Hz
				Pulse width	12.9 ms
				Scanning speed	5.43 mm/s
Guofu Lian 2018 [86]	AISI/SAE 1045 steel	W6Mo5Cr4V2 powder	Multi-track clad width, flatness ratio, dilution rate	Laser power	1.5 kW
				Scanning speed	6 mm/s
				Gas flow	1018.81 L/h
				Overlap rate	23.47%
Sha Wu 2021 [87]	42CrMo alloy	Ni60A-25% WC powder	Dilution rate, unit effective area	Laser power	2799.93 W
				Scanning speed	236.84 mm/min
				Powder feeding rate	5 g/min
				Spot diameter	3 mm

As a traditional optimization method, the response surface methodology has been successfully applied to various system optimization problems, especially to multivariate response problems. However, the premise of an experimental design using this method is that the designed experimental sites should contain optimal conditions. Otherwise, the optimization results will be biased. Therefore, reasonable experimental factors and levels must be determined when optimizing the response surface methodology.

2.4. Taguchi Method

The Taguchi method is a low-cost, high-efficiency experimental design method used in many engineering problems [88]. In the Taguchi method, orthogonal arrays can effectively determine the influence of variables and levels to achieve robust designs, which can significantly reduce the experimental time and cost [89].

Due to the simplicity and clarity of the experimental design method of the Taguchi method, in recent years, the Taguchi method has become a powerful tool to improve productivity in the R&D stage [90]. Xu et al. [91] investigated the effect of the process parameters on bond shear strength and microhardness using the Taguchi method. They found that the powder type had the most significant effect on the bond strength. Quazi et al. [92] improved the tribomechanical properties of a Ni-WC composite coating on the surface of AA5083 aluminum alloy by using the Taguchi method to optimize the laser cladding process parameters. The results show that the laser power, defocus amount, and scanning speed significantly affect the surface hardness and wear resistance.

Some scholars have improved the Taguchi method and proposed the mixed Taguchi method. Chen [93] and Shi et al. [94] combined the Taguchi method with the empirical statistical model and TOPSIS methods. The results show that both methods can significantly improve the microhardness of coatings. Zhang [95], Paul [96], Deng [97], and Yu et al. [98] combined grey correlation analysis and the Taguchi method to optimize the process parameters. This method can simplify complex multi-parameter optimization to a single-objective optimization problem, which significantly reduces the difficulty of optimization. The optimized cladding layer obtained by this method is significantly better than other cladding layers in terms of morphology and microstructure, which also verifies the feasibility of Taguchi's grey correlation method. A grey relational graph of the process parameters; the influence of the process parameters on the cladding's height, width, and

dilution SNR; and the cross-sectional metallographic structure comparison of the specimen before and after optimization are shown in Figure 4.

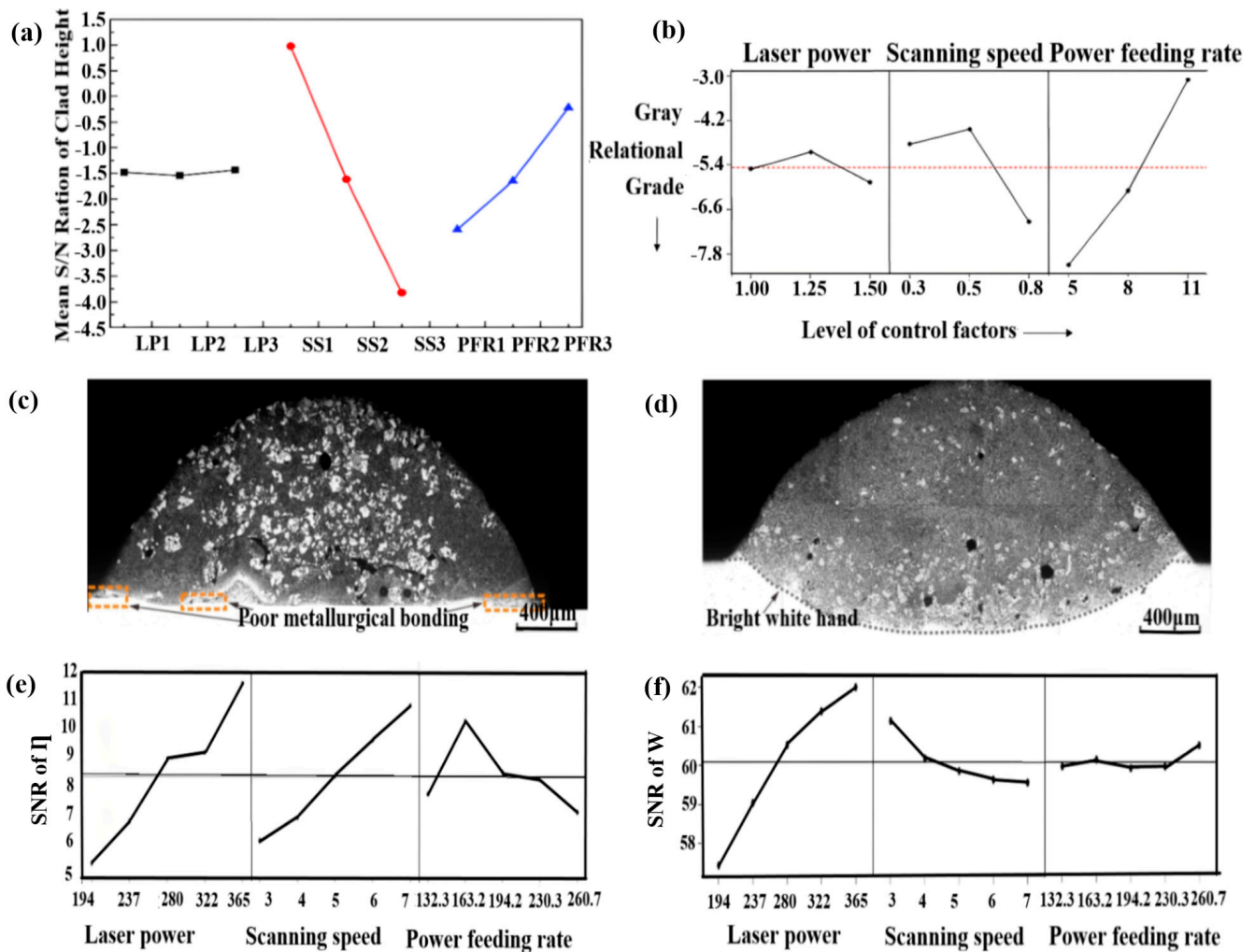


Figure 4. A grey relational graph of the process parameters, the influence of processing parameters on the signal-to-noise ratio of cladding, and the metallographic microstructure comparison of specimen cross-sections before and after optimization. (a) Effects of processing parameters on the S/N ratio of clad height. Reprinted with permission from Ref. [95]. 2016, Springer Nature. (b) Graph of grey relational grade. Reprinted with permission from Ref. [96]. 2013, Springer Nature. (c) Metallographic microstructure of the specimen cross-section under initial parameters. Reprinted with permission from Ref. [97]. 2022, Elsevier. (d) Metallographic microstructure of specimen cross-section under optimal parameters. Reprinted with permission from Ref. [97]. 2022, Elsevier. (e) Main effects plot for SNR of the dilution rate. Reprinted with permission from Ref. [98]. 2018, Elsevier. (f) Main effects plot for SNR of the clad width. Reprinted with permission from Ref. [98]. 2018, Elsevier.

Although the Taguchi method is a cost-effective experimental design, it must indicate the test. The best combination can only be a combination of a specific test level. The optimal solution can only be within the range of the chosen level. When an interaction between controllable factors is apparent, it can lead to inaccurate results from ANOVA.

2.5. Other Traditional Optimization Methods

In addition to optimization methods such as the response surface methodology, regression analysis, single-factor experiments, and Taguchi method, traditional optimization methods such as orthogonal experiments, principal component analysis, TOPSIS, grey

relational analysis, the improved analytic hierarchy process approach, theoretical–empirical models, the desirability function approach, and Design Expert statistical software are also used to optimize the laser cladding process parameters.

Peng et al. [99] used the coating’s average hardness value and dilution ratio as evaluation indexes and obtained the optimal process parameters through orthogonal experiments. Marzban [100] and Wang et al. [101] combined principal component analysis (PCA) with the TOPSIS method and grey correlation relationship analysis, respectively. They achieved the multi-response optimization of the laser cladding process. Liang et al. [102] proposed a laser cladding coating quality evaluation method based on fuzzy comprehensive evaluation (PCE) and an improved analytic hierarchy process (IAHP) approach. The results show that the method can help to optimize the process parameters. Reddy et al. [103] studied the influence of the process parameters on the powder deposition efficiency, dilution, and porosity by establishing a theoretical–empirical model. The experimental results show that the laser power and powder feeding rate greatly influence the deposition efficiency and dilution, and the porosity is mainly related to the raw material. Meng [104], Menghani [105], Mohammed [106], and Liu et al. [107] used the desirability function approach to identify the optimum magnitude of the process parameters in the laser cladding process to obtain better cladding quality and geometry. Rasheedat [108] and Moradi et al. [109] designed a complete factorial experiment, ran many experiments with different process parameters, and obtained the best process parameters through the Design Expert statistical software. Table 3 lists the optimization methods and evaluation indexes. The microstructure at the optimum process parameters and a comparison with the substrate microstructure are shown in Figure 5. It can be seen from the figure that the coating and substrate bond well at the optimum process parameters. In addition, many equiaxed dendrites were formed at the top of the coating, the cladding layer was uniform and compact, the overall quality was good, and the wear resistance was improved. Compared to the substrate, the wear mechanism of the coated specimen changed to abrasive wear.

Table 3. The optimization methods and evaluation indexes.

Authors [Year/Reference]	Optimization Method	Substrate	Cladding Material	Evaluation Indexes	Process Parameters	Optimal Process Parameters
Pengfei Fan 2020 [99]	Orthogonal experiments	15 MnNi4M o steel	Co50 powder and WC powder	Clad depth, clad width, clad height, dilution rate, hardness	Laser power	2.4 kW
					Powder feeding rate	0.5 g/s
					Scanning speed	7 mm/s
Javad Marzban 2015 [100]	PCA with TOPSIS	AISI 1040	Ni-Cr-Mo powders	Clad height, clad width, clad depth	Laser power	1 kw
					Powder feeding rate	8 mg/min
					Scanning speed	0.5 m/min
Qianting Wang 2020 [101]	PCA with GRA	AISI 1045	Fe50 powder and TiC powder	Clad width, flatness, non-fusion area	Laser power	1.77 KW
					Power ratio	35.28%
					Overlapping ratio	24.06%
					Defocus amount	−0.44 mm
Wanxu Liang 2021 [102]	FCE with IAHP	45 steel	316 L stainless steel powder	Coating profile, microstructure, mechanical properties	Laser power	≤1200 W
					Scanning speed	5~7 mm/s
					Overlap rate	30~40%
L. Reddy 2018 [103]	Theoretical– empirical model	15Mo3	SHS 7170 powder	Powder deposition efficiency, dilution, porosity	Laser power	1000 W
					Powder feeding rate	4 g/min
					Scanning speed	300 mm/min

Table 3. Cont.

Authors [Year/Reference]	Optimization Method	Substrate	Cladding Material	Evaluation Indexes	Process Parameters	Optimal Process Parameters
Jyoti Menghani 2021 [105]	Desirability function approach	AISI 316	AlFeCuCrCoNi high-entropy powder	Clad height, clad depth, clad width, percentage dilution	Laser power	1.1 kW
					Powder feeding rate	4 g/min
					Scanning speed	500 mm/min
Mahmoud Moradi 2021 [109]	Design Expert statistical software	4130 alloy steel	Inconel 718 powder	Clad height, clad width, standard deviation of microhardness, the stability of additively manufactured walls	Scanning speed	2.5 mm/s
					Powder feeding rate	28.52 g/min
					Scanning strategies (unidirectional, bidirectional)	Unidirectional

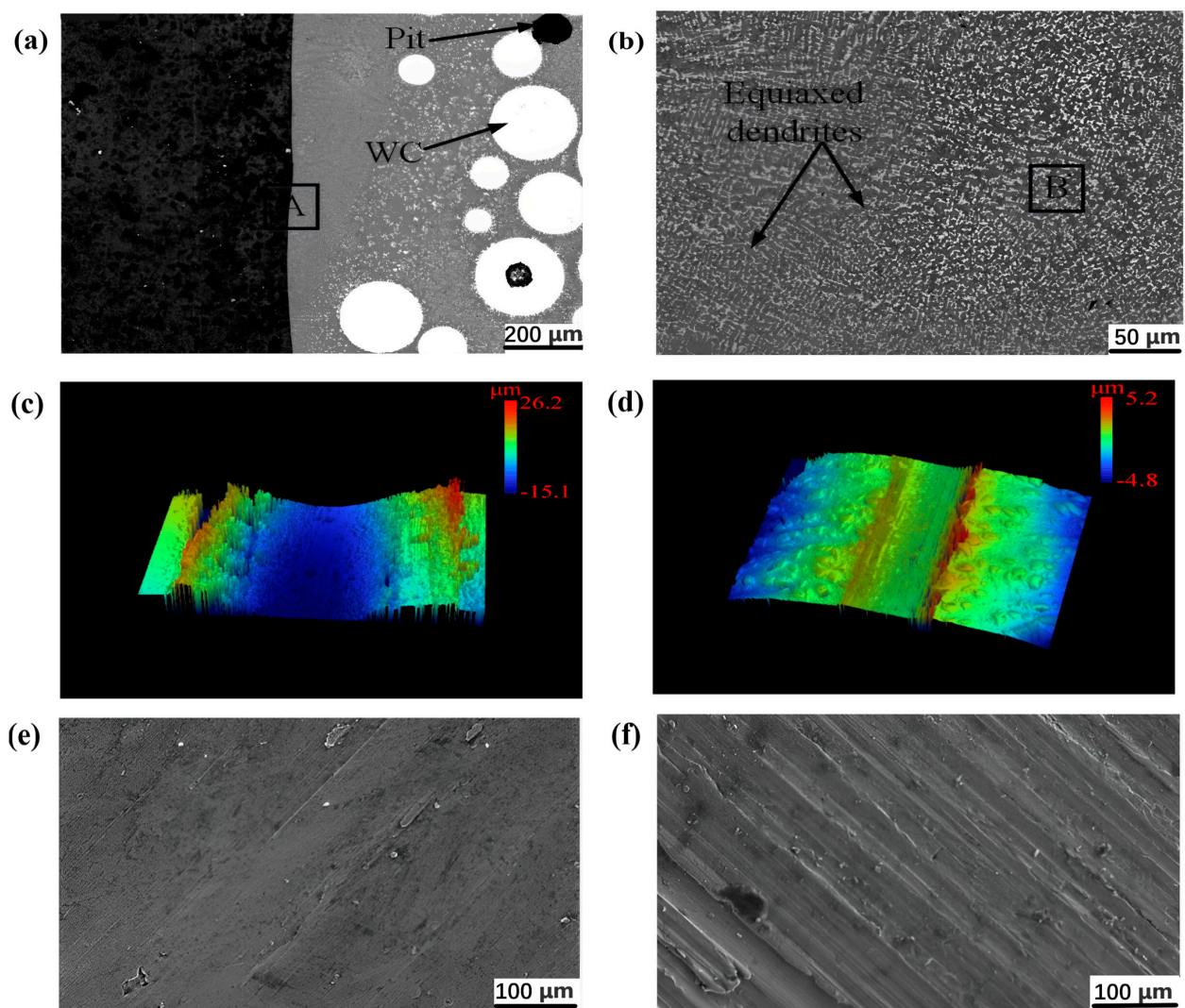


Figure 5. The microstructure at optimum process parameters and a comparison with the substrate microstructure. (a) Microstructure of the lower part of the cladding layer. Reprinted with permission from Ref. [99]. 2020, Elsevier. (b) Microstructure of the top of the cladding layer. Reprinted with permission from Ref. [99]. 2020, Elsevier. (c) 3D worn morphologies of substrate. Reprinted from [101]. (d) 3D worn morphologies of optimized clad layer [101]. (e) SEM morphologies of worn surfaces for HEA clad SS-316 at optimum process parameters. Reprinted from [105]. (f) SEM morphologies of worn surfaces for untreated SS-316 [105].

Traditional optimization methods are often specific to a given process, without considering physical changes such as thermal strain and the cooling rate during optimization. Optimization methods still need to be redesigned when new materials or processes are used, and extensive experiments are performed to optimize the process parameters. In addition, the use of traditional optimization methods often requires a specific mathematical foundation, and some mathematical operations are necessary for the optimization process and the mathematical analysis of the experimental results.

3. Intelligent Optimization Methods

3.1. Artificial Neural Network Model

The artificial neural network is a robust empirical modeling tool with significant advantages, such as high accuracy, low costs, and short times, and it is one of the most applicable models in non-linear analysis [110]. It has a high degree of non-linear fitting capability, which is impossible with traditional methods [111]. Among them, the BP neural network is well suited for physical applications, and it is currently one of the most widely used artificial neural networks [112,113].

In recent years, the artificial neural network has made remarkable achievements in materials science. It has begun to be applied to laser cladding to predict the cladding layer morphology and optimize the process parameters [114–116]. Song et al. [117] found, through an experimental comparison, that the artificial neural network model is more suitable for describing the non-linear relationship between process parameters and cladding geometry than the response surface model. Li et al. [118] used the BP neural network to establish a laser cladding AlCoCrFeNi coating dilution rate prediction model; they found that under the optimum process parameters, the coating microstructure was composed of a simple BCC solid solution phase, the grains were equiaxed, and no serious segregation of internal elements occurred. Thus, the coating crack could be effectively controlled. Caiazzo et al. [119] used an artificial neural network to study the relationship between the laser cladding process parameters and cladding layer size. The results show that this method can obtain the required process parameters for specific cladding layer sizes. Guo et al. [120] used the BP neural network model to study the influence of the process parameters on the coating quality of a high-power semiconductor laser cladding cobalt-based alloy. The results showed that the width, height, and depth of the cladding layer were related to the laser scanning speed, and the hardness of the cladding layer was related to the powder feeding rate. The neural network prediction errors are shown in Table 4. The BP neural network training process, a comparison between the BP neural network model and the RSM model prediction results, and the microstructure of AlCoCrFeNi HEA coatings under the optimal process parameters are shown in Figure 6.

Table 4. Neural network prediction objects and errors.

Authors [Year/Reference]	Substrate	Cladding Material	Optimization Method	Prediction Error		
Changhui Song 2020 [117]	316 L stainless steel	316 L stainless steel powder	BPNN	Clad wight 2.79%	Clad height 3.09%	
Yutao Li 2021 [118]	40CrNiMo alloy steel	AlCoCrFeNi high-entropy alloy powder	BPNN	Dilution rate 5.89%		
Fabrizia Caiazzo 2018 [119]	2024 aluminum alloy	2024 aluminum alloy powder	ANN	Laser power 2.0%	Scanning speed 5.8%	Powder feeding rate 5.5%

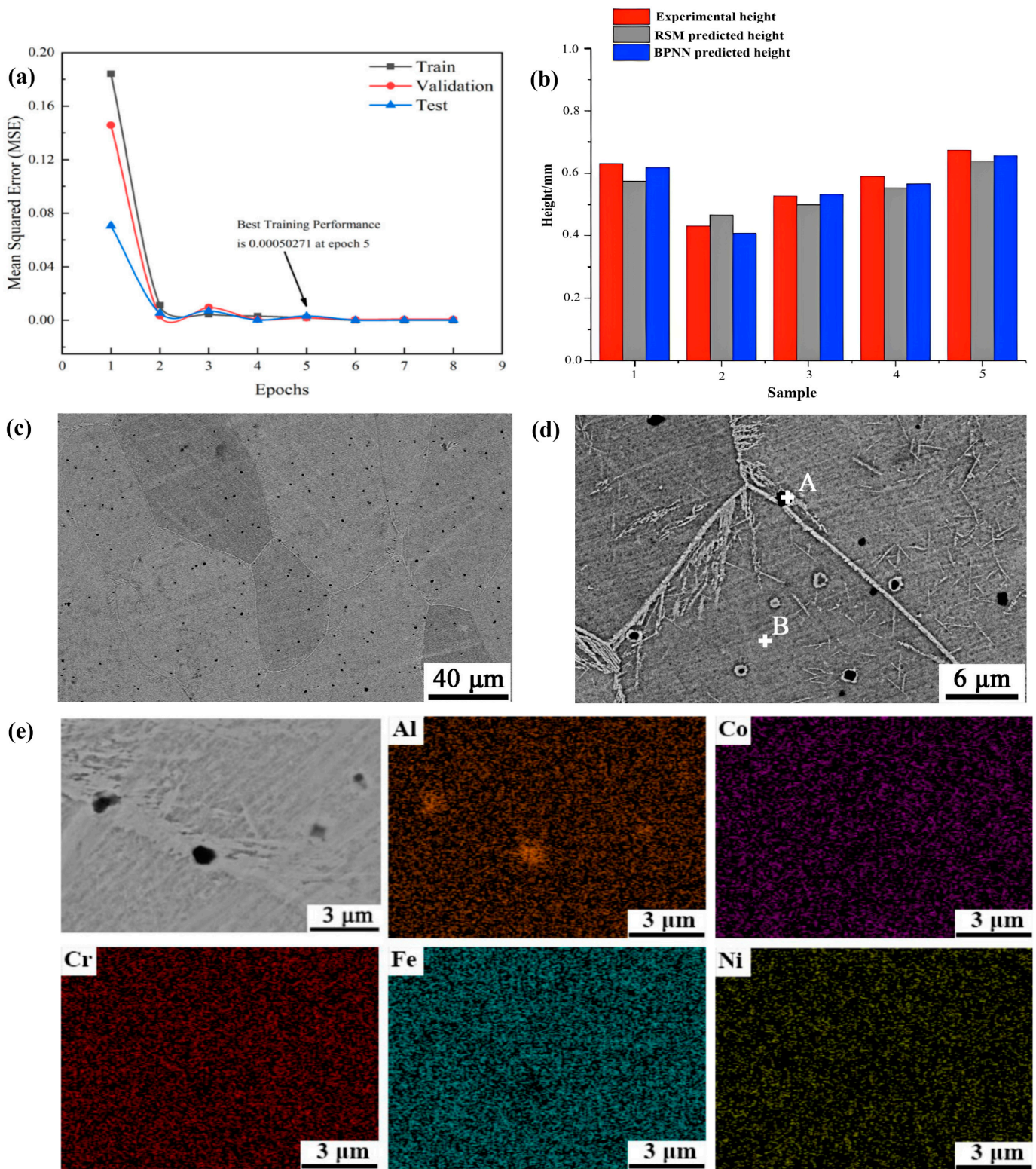


Figure 6. The BP neural network training process, the comparison between the BP neural network model and the RSM model prediction results, and the microstructure of AlCoCrFeNi HEA coatings under optimal process parameters. (a) The BP neural network training process. Reprinted from [118]. (b) Comparison of the prediction results of neural networks and RSM for clad height. Reprinted with permission from Ref. [117]. 2020, Elsevier. (c) Back-scattered SEM images of the AlCoCrFeNi coating

microstructure under low magnification [118]. (d) Back-scattered SEM images of the AlCoCrFeNi coating microstructure under high magnification. At the region marked B in (d), the Fe element content was the highest, which was 30.40 at.%; and the Al element content was the lowest, which was 14.98 at.%. The black granular microstructure (marked A) had the highest content of Al and N elements, which were 38.41 at.% and 25.23 at.%, which indicates that the particles were the AlN phase. [118]. (e) EDS maps of AlCoCrFeNi coating [118].

A neural network is suitable for handling large data samples, and when the number of samples is too small, the results may need to be more accurate. In addition, neural network models tend to fall into local minima and take longer to learn and train. Therefore, there is a need to apply more optimization algorithms to the neural network.

3.2. Genetic Algorithm Optimizes BP Neural Network (GABP)

The genetic algorithm is a non-traditional optimization tool based on random search techniques [121]. The genetic algorithm has a good global optimization ability, which is suitable for dealing with multi-objective problems [122,123]. The artificial neural network has a long learning time and slow convergence speed, and quickly falls into local minima [124]. Its combination with genetic algorithms can effectively optimize the threshold value of the neural network and achieve a fast global optimization search [125].

Liu et al. [126] found that GABP neural networks have higher prediction accuracy than BP neural networks. At the same time, the combination of a double hidden layer and single-output neural network led to higher prediction accuracy. Pang et al. [127] found that the GABP neural network had better optimization ability than the response surface method. The process parameters obtained using the GABP neural network could improve the deposition rate for laser cladding. Huang [128] and Yang et al. [129] combined genetic algorithms with a neural network model to study the relationship between the laser cladding process parameters and cladding layer quality. The results show that the optimization method can be applied to the crack control of laser cladding molding and can provide some references for the optimization of the laser cladding process parameters. The GABP predictions and their comparison with the BPNN predictions are shown in Figure 7.

The programming implementation of genetic algorithms is complex. The search speed of the algorithm could be faster and requires a long training time. There are better solutions than a single genetic algorithm for large-scale computational problems, and they can easily fall into premature convergence.

3.3. Support Vector Machines (SVM)

Support vector machines (SVM) are a statistical learning method based on structural risk minimization. Support vector regression (SVR) is a vital application branch of support vector machines (SVM). Compared with artificial neural networks, SVM still has a strong generalization ability and global optimization ability when the training data are insufficient. In recent years, it has become a hotspot in various research and industrial process applications and has been successfully applied to modeling and regression analysis problems [130–133].

Chen et al. [134] used the support vector machine (SVM) model to study the influence of the process parameters on the coating quality characteristics. The results show that the preset powder thickness, laser spot diameter, and power are the most critical process parameters. Chen et al. [135] established a multi-output support vector regression (M-SVR) model. Through experiments, they found that its accuracy was higher than that of the single-output support vector regression (S-SVR) model and the BP neural network model. Yao et al. [136] established a support vector regression (SVR) model based on the Gaussian radial (RBF) kernel function. This model is more accurate than the BP neural network model and can help to select the process parameters. Zhang et al. [137] optimized the process parameters by combining the multi-objective slime mold algorithm (MOSMA) and support vector regression (SVR). The results show that compared with other methods, such as the response surface methodology, the best process parameters obtained by this

method can lead to coatings with better performance. A comparison of the prediction results of support vector regression and the BP neural network is shown in Table 5. The prediction model framework for support vector machines, a comparison of the predicted and experimental values for SVR, and a comparison of the predicted values for SVR and BPNN are shown in Figure 8.

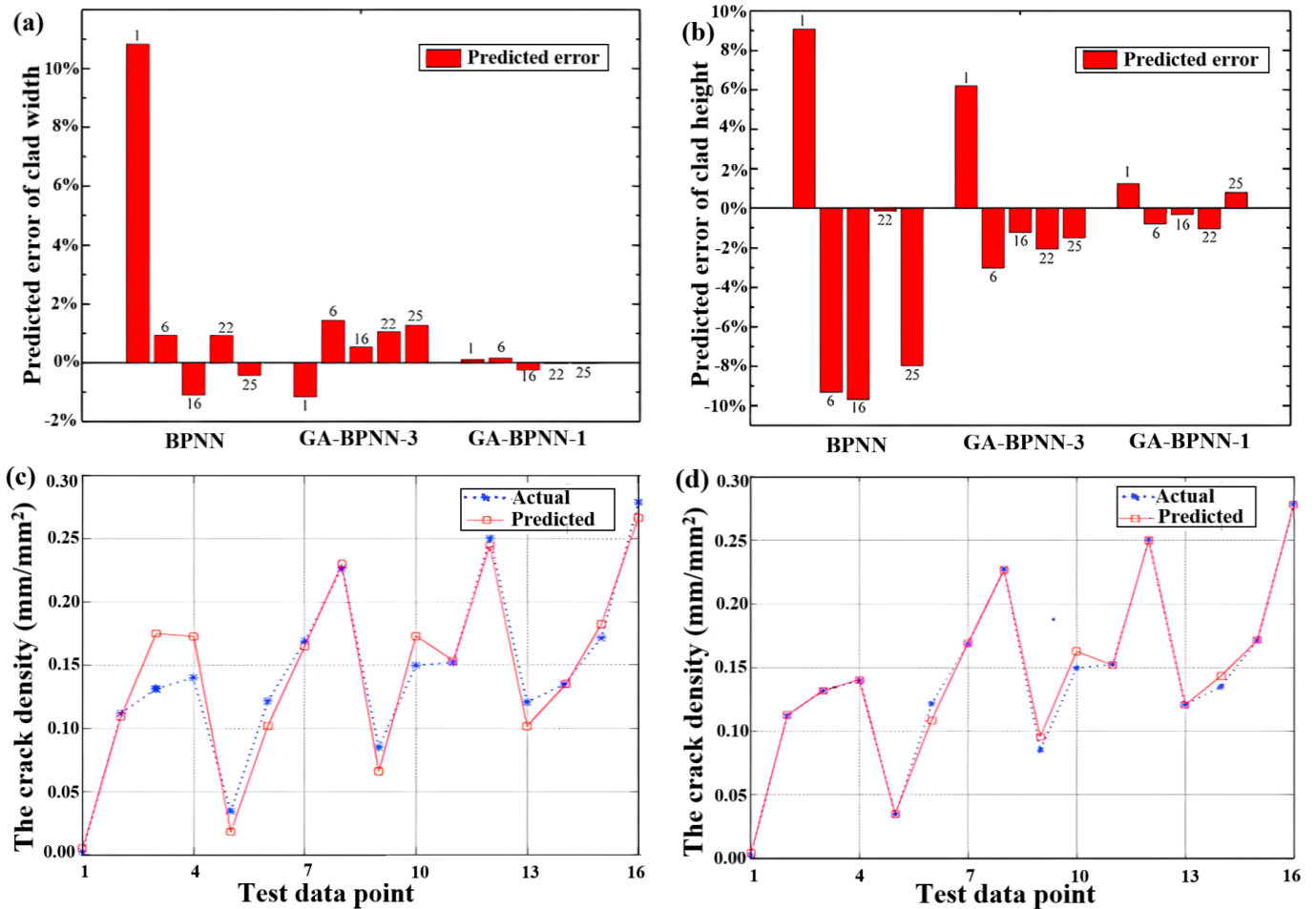


Figure 7. The GABP predictions and their comparison with the BPNN predictions. (a) Comparison of the prediction error of the triple-output-layer GABPNN with the single-output-layer GABPNN and BPNN for the clad width. Reprinted with permission from Ref. [126]. 2018, Springer Nature. (b) Comparison of the prediction error of the triple-output-layer GABPNN with the single-output-layer GABPNN and BPNN for the clad height. Reprinted with permission from Ref. [126]. 2018, Springer Nature. (c) Prediction results of BPNN [128]. (d) Prediction results of GABP [128].

Support vector machines (SVM) can effectively solve regression problems and perform well when dealing with small sample data. However, they are only suitable when processing a small amount of data, and, when there are too many data sets, they require a long time to solve the problem and show poor results.

Table 5. Comparison of support vector regression and BP neural network prediction results.

Authors [Year/Reference]	Substrate	Cladding Material	Optimization Method	Prediction Error	
				Clad width	Clad height
Xiyi Chen 2021 [135]	316 L stainless steel	316 L stainless steel powder	BPNN	15%	6%
			M-SVR	5%	5%
Yao Wang 2020 [136]	316 L stainless steel	Fe powder	BPNN	6.72%	7.96%
			RBF-SVR	4.58%	5.33%

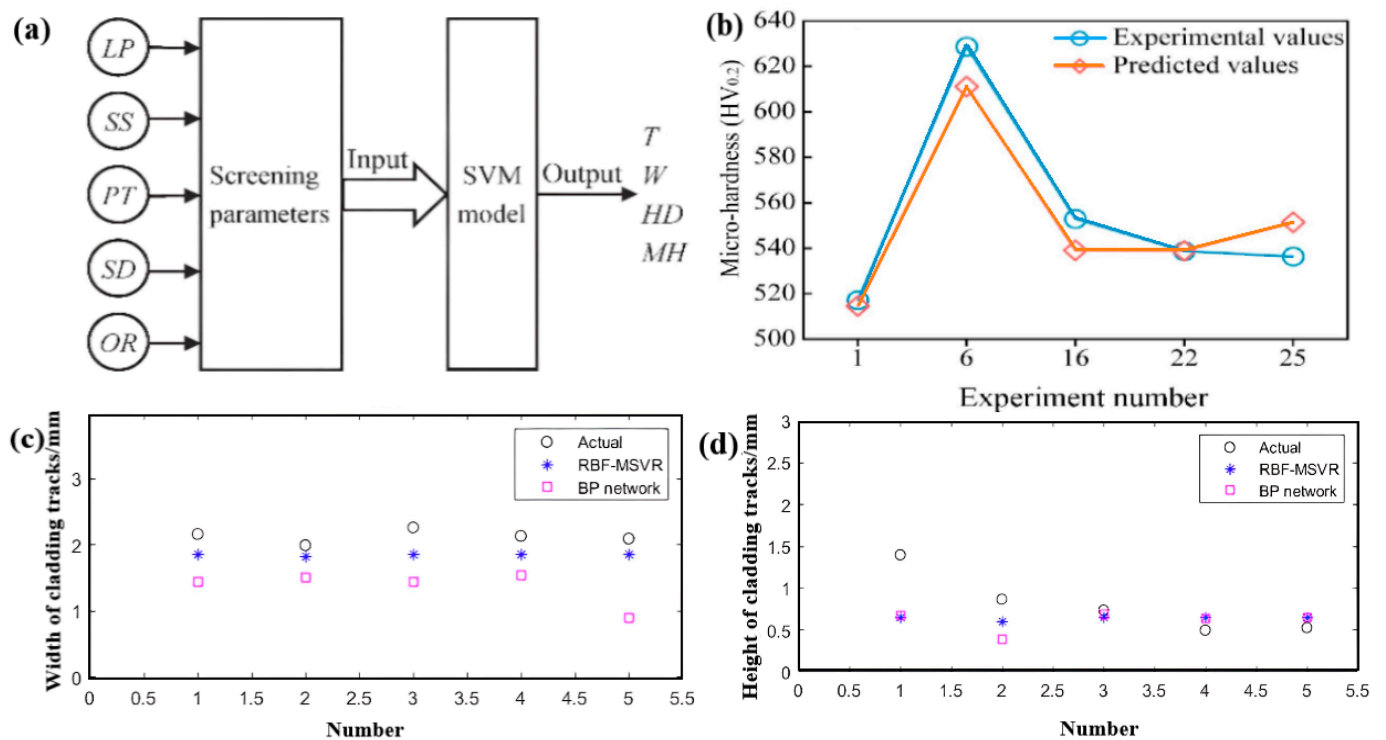


Figure 8. A prediction model framework for support vector machine, comparison of predicted and experimental values of SVR, and comparison of the predicted values of SVR and BPNN. (a) The prediction model framework of the support vector machine. Reprinted with permission from Ref. [134]. 2019, Elsevier. (b) Predicted results for microhardness and experimental values. Reprinted with permission from Ref. [134]. 2019, Elsevier. (c) Comparison of the predicted values of the clad width of SVR and BPNN [135]. (d) Comparison of the predicted values of the clad height of SVR and BPNN [135].

3.4. Novel Non-Dominated Sorting Genetic Algorithm II (NSGA-II)

The novel non-dominated sorting genetic algorithm II (NSGAI) is a well-known meta-heuristic that can effectively solve non-linear multi-objective optimization problems [138]. It has the advantages of fast operation and good solution convergence.

Peng et al. [139] used a hybrid TS-GEP algorithm and NSGA-II to optimize the laser cladding process parameters. By using this method, they improved the energy and material utilization rate in the laser cladding process. Jiang [140] and Lin et al. [141] optimized the laser cladding process parameters using the NSGA-II algorithm. The results show that this

method can effectively reduce the energy loss in the laser cladding process and improve the macro quality and microhardness of the cladding layer. Zhao et al. [142] used the NSGA-II algorithm to optimize the process parameters for coaxial powder-feeding laser cladding. The results showed that the use of the optimized parameters could reduce the depth of the heat-affected zone of the substrate and improve the cladding efficiency. The results of the response values before and after optimization using the NSGA-II algorithm are shown in Table 6.

Table 6. Comparison of response values before and after NSGA-II optimization.

Authors [Year/Reference]	Substrate	Cladding Material	Response Values before and after Optimization				
			Response	Energy consumption (J)	Powder utilization	Microhardness (HV)	Aspect ratio
Xingyu Jiang 2022 [140]	45 steel plate	304 L powder	Response	Energy consumption (J)	Powder utilization	Microhardness (HV)	Aspect ratio
			Before	2,972,340.405	43%	221	3.6
			After	1,798,861.43	46%	235	4.5
Linsen Shu 2022 [141]	TC4 plate	TC4 alloy powder	Response	Wear depth (μm)	Wear width (μm)	Microhardness (HV)	Average mean friction coefficient
			Before	74.54	2459.64	429.5	0.374
			After	56.64	1884.79	473.3	0.293
Zhao Kai 2020 [142]	20 steel	Inconel 625 powder	Response	Efficiency ($\text{mm}^2 \cdot \text{s}^{-1}$)	Heat- affected zone depth	Microhardness (HV)	Dilution
			Before	15.24	0.855	186.433	0.518
			After	16.17	0.736	218.337	0.32

The NSGA-II algorithm can achieve good results in low-dimensional multi-objective optimization problems. However, for high-dimensional multi-objective optimization problems, when there are too many optimization goals, the selection pressure will be too small, and the computational complexity will increase significantly. Therefore, the algorithm needs to continue to be improved.

3.5. Particle Swarm Optimization Algorithm (PSO)

Particle swarm optimization (PSO) is a class of metaheuristic search algorithms without derivatives [143]. The mode of operation of particle swarm algorithms is similar to that of genetic algorithms. However, particle swarm algorithms consider individuals in the form of populations, rather than focusing only on a single individual, as genetic algorithms do [144]. They are widely used in multi-objective optimization problems because of their fast convergence, simple operation, and few parameters [145].

Pant et al. [146] developed a prediction model considering the process parameters and powder capture efficiency, clad height, and width using the particle swarm algorithm to optimize the artificial neural network. The results showed that the PSO-ANN model's prediction results were more accurate than those of the ANN model. Deng et al. [147] developed a BPNN-QPSO neural network prediction model for the laser cladding of Ti (C, N) ceramic coatings and compared the method with the Taguchi method, BPNN, and BPNN-PSO. The results show that the probability of the BPNN-QPSO model falling into the locally optimal solution is low, and the convergence speed is fast. Ma et al. [148] used a multi-objective quantum particle swarm optimization algorithm to find the minimum dilution rate and residual stress. They found that the defocus amount had the most excellent effect on the dilution rate, and the scanning speed had the most significant impact on the residual stress. Chukwubuike et al. [149] used particle swarm optimization algorithms to optimize individual objective functions, obtained the optimal process parameters, and developed

a user interface through which the parameters could be optimized directly using particle swarm optimization, without redesigning the optimization methods. Figure 9 shows a comparison of the performance of the neural network and the particle swarm optimization neural network models, and an iterative comparison of the coatings' microhardness fitness values under different optimization methods.

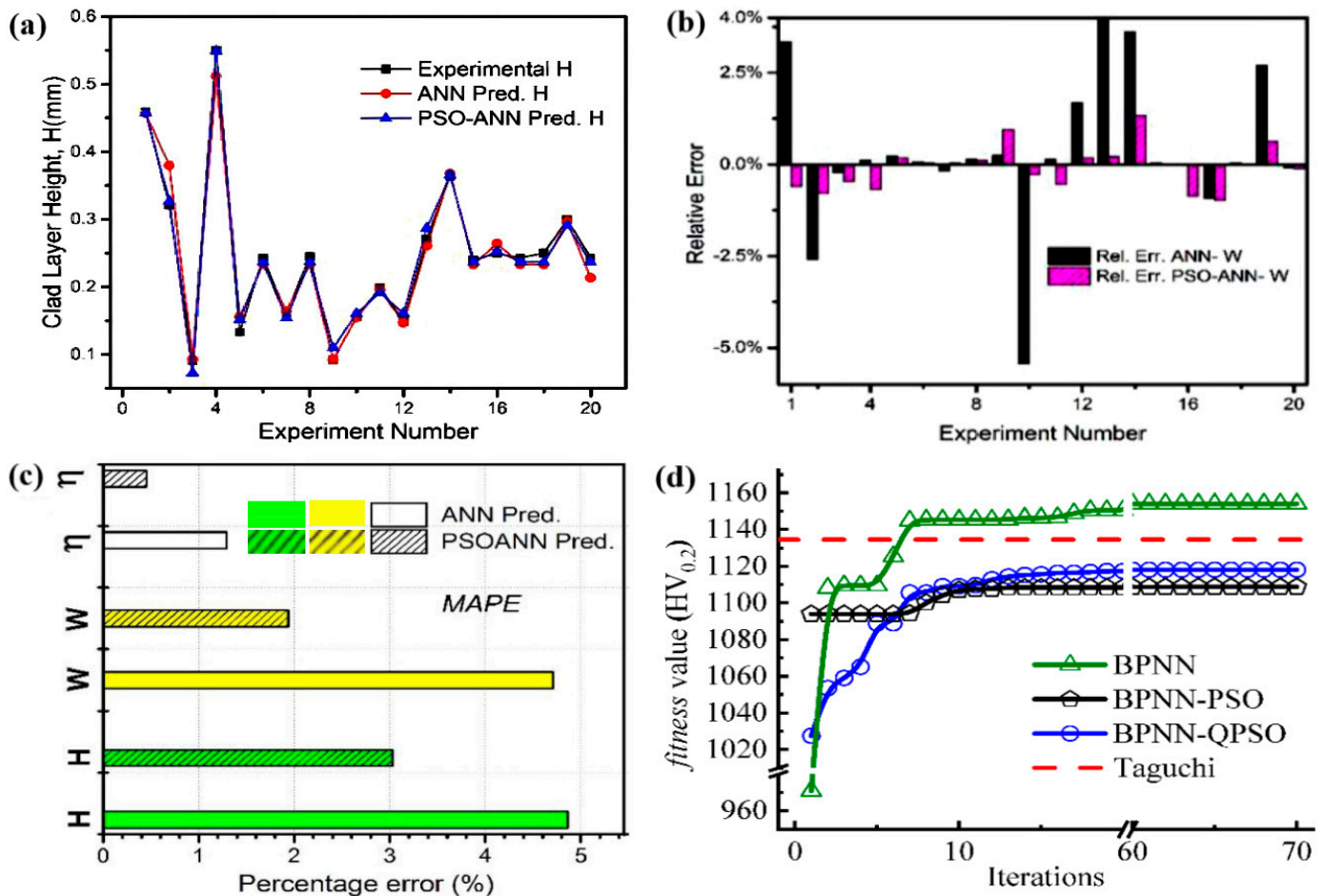


Figure 9. Performance comparison of a neural network model optimized by the particle swarm algorithm with a neural network model. (a) Comparison of experimental and ANN and PSO-ANN models' predicted results for clad height. Reprinted with permission from Ref. [146]. 2020, Elsevier. (b) Relative error of ANN and PSO-ANN models for clad width. Reprinted with permission from Ref. [146]. 2020, Elsevier. (c) Performance comparison between the neural network and the PSOANN model. Reprinted with permission from Ref. [146]. 2020, Elsevier. (d) The iterative comparison of the coating microhardness fitness values under different optimization methods [147].

The standard PSO algorithm may sometimes fail to converge to the optimal global solution. The multi-objective QPSO algorithm is superior in terms of convergence speed and accuracy compared to the standard PSO algorithm. However, the multi-objective QPSO algorithm that converges too quickly may lead to premature convergence, reducing the convergence accuracy.

3.6. Other Intelligent Optimization Methods

The most commonly used intelligent optimization algorithms in laser cladding are the neural network, GABP, support vector machines (SVM), and particle swarm algorithms (PSO). However, in addition to these algorithms, algorithms such as the adaptive neuro-fuzzy inference system (ANFIS), random forest (RF), grey wolf optimization (GWO), and the Bonobo optimization algorithm have also been applied to laser cladding.

Singh et al. [150] used four different methods (sine cosine algorithm, coyote optimization algorithm, Jaya algorithm, and Bonobo optimization algorithm) to optimize the process parameters in order to obtain the minimum dilution. They found that the Bonobo optimization algorithm converged the fastest when searching for the global optimum solution. At the optimum parameters, the microhardness of the clad layer was significantly increased due to the diffusion of WC particles during the cladding process. Zhou et al. [151] determined the optimal process parameters by combining the grey wolf optimization algorithm and the BP neural network. They found that the GWO-BPNN model was more accurate than the predictions of the BPNN model. Under the optimum process parameters, the wear resistance and corrosion resistance of the cladding layer were significantly improved, with wear in the form of adhesion and fatigue wear. Sohrabpoor et al. [152] optimized the process parameters by correlating the ANFIS response model with the Imperialist Competition Algorithm (ICA). The results show that the method effectively improves the powder collection efficiency and obtains the desired clad height and clad width. Liang et al. [153] used a random forest algorithm to construct a regression model of laser cladding process parameters (laser power, scanning speed, powder feeding rate) and a single-pass cladding layer size. The results show that this method can accurately estimate the laser cladding process parameters required to process the cross-sectional geometry of a specific single-pass cladding layer. The prediction results of ANFIS, RF optimization methods, and GWO optimization of BPNN before and after their application are shown in Table 7. The results of the optimized microstructure are shown in Figure 10.

Table 7. The prediction results of ANFIS, RF optimization methods, and GWO optimization of BPNN.

Authors [Year/Reference]	Substrate	Cladding Material	Optimization Method	Predicted Error		
				Clad height MSE (10 ⁻³)	Clad weight MSE (10 ⁻³)	Dilution MSE (10 ⁻³)
Zhijie Zhou 2022 [151]	20Cr13 stainless steel	15-5PH powder	BPNN	1.053	0.642	4.969
			GWO- BPNN	0.161	0.715	0.267
Hamed Sohrabpoor 2016 [152]	A36 mild steel	Fe-based alloy powder	ANFIS	Powder catchment efficiency 7.62%	Clad height 8.36%	Clad width −3.83%
Liang Xudong 2020 [153]	Stainless steel	Inconel 625 powder	RF	Laser power 1.17%	Scanning speed 3.43%	Powder feeding rate 3.51%

At present, intelligent optimization algorithms have begun to be applied to laser cladding, but there are still some limitations. Optimizing the process parameters using intelligent optimization methods often requires extensive experimentation to obtain valid training data, which can also increase the costs. Moreover, a single intelligent algorithm will likely produce local convergence, failing to obtain the optimal process parameters. Therefore, in the future, hybrid intelligence algorithms should be used more often to optimize the process parameters.

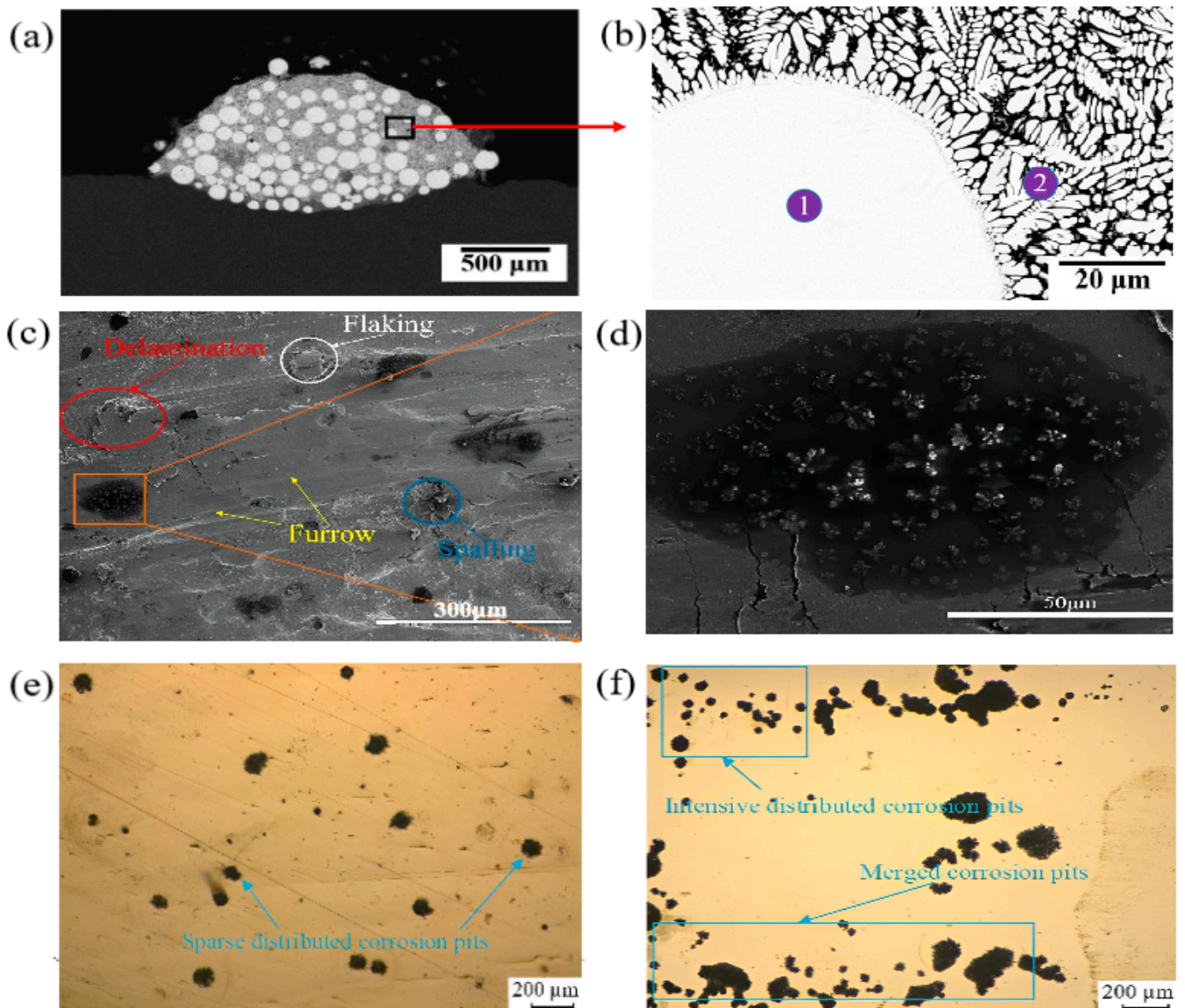


Figure 10. Microstructure of the cladding layer under optimal parameters, frictional wear properties, and corrosion resistance. (a) BSD image of the clad cross-section with optimal parameters. Reprinted with permission from Ref. [150]. 2021, Elsevier. (b) Microstructure of the cladding section with optimal parameters. 1 and 2 are showing spots for further EDS analysis. Reprinted with permission from Ref. [150]. 2021, Elsevier. (c) SEM image of the worn surface of a 15-5PH cladding layer under high magnification [151]. (d) SEM image of the worn surface of a 15-5PH cladding layer under low magnification [151]. (e) SEM image of 15-5PH cladding layer after electrochemical corrosion experiments [151]. (f) SEM image of 20Cr13 substrate after electrochemical corrosion experiments [151].

4. Summary and Outlook

It can be seen from the above that the optimization of the process parameters of laser cladding is a complex multi-parameter optimization problem. Through the optimization of the laser cladding process, the parameters can effectively improve the quality of the coating. With the deepening of research, many optimization methods have been developed. In the early years, more traditional optimization methods were used. However, with the development of computer technology, intelligent algorithms began to be applied to optimization problems, but these optimization methods still have some defects. The authors

believe that the future development trend of process parameter optimization methods is as follows.

4.1. A Deeper Look at Intelligent Algorithms

Intelligent algorithms have recently been widely used in various optimization fields. However, there are still relatively few applications for evolutionary algorithms in laser cladding, such as simulated annealing algorithms, ant colony algorithms, prohibited search algorithms, and artificial bee colony algorithms. Convolutional neural networks and radial basis neural networks are rarely reported. There are many other areas where improvements to the non-dominated sorting second-generation algorithm have been reported to significantly improve the algorithm's performance. However, they have yet to be widely used in laser cladding. In addition, since hybrid intelligence algorithms can overcome the shortcomings of single algorithms, more research into hybrid algorithms should follow as well.

4.2. Optimization of Process Parameters under External Auxiliary Conditions

There are many reports that external conditions such as ultrasound and electromagnetic fields can effectively improve the quality of coatings. However, only a few scholars have investigated their effect in optimizing the process parameters. The optimization of the process parameters under external auxiliary conditions can be analyzed to optimize the process parameters more successfully and prepare better coatings with superior properties.

4.3. Optimization Studies Carried out on More Parameters, and More Evaluation Indicators Introduced

There are many process parameters in laser cladding. However, many scholars only optimize and study process parameters such as the laser power, scanning speed, and powder feeding rate. More research needs to be carried out to optimize other process parameters. The laser cladding results are generally evaluated by performance indicators such as the cladding width, height, depth, dilution rate, wear resistance, microhardness, etc. In contrast, the mechanical properties of the coating, such as bending, tensile, fatigue, compression, and shear properties, are rarely studied. It is essential to strengthen the research on the optimization of other process parameters and introduce more evaluation indicators to study the laser cladding process parameters.

4.4. Development of Software That Allows the Optimization of Laser Cladding Process Parameters

Both traditional and intelligent optimization methods require many experiments, which can waste time and increase costs. Developing software that can intelligently select the best process parameters is essential.

Author Contributions: Conceptualization, formal analysis and writing—original draft, K.W., W.L., J.J. and Y.T.; writing—original draft preparation, K.W. and W.L., Methodology, data curation and funding acquisition, K.W., M.Z. and H.F.; Project administration and supervision, K.W. and Y.T.; Data analysis, writing—review and editing, H.M.S.S., Y.H. (Yuxiang Hong), Y.H. (Yongle Hu), J.Z. and D.X. All authors have read and agreed to the published version of the manuscript.

Funding: The authors would like to acknowledge the financial support for this work from the National Natural Science Foundation of China (52205334), the Natural Science Foundation of Hunan Province (2022JJ40495), the Changsha Key Research and Development Project (kh2201275), the Changsha Municipal Natural Science Foundation (kq2202196), the R&D Program of Beijing Municipal Education Commission (KZ202210005004), the Open Fund of Key Laboratory of Intelligent Manufacturing Quality Big Data Tracing and Analysis of Zhejiang Province (ZNZZSZ-CJLU2022-02), the Tribology Science Fund of State Key Laboratory of Tribology in Advanced Equipment (SKLTKF21B08), and the Open Fund of Key Laboratory of Vibration and Control of Aeropropulsion System (VCAME202213).

Institutional Review Board Statement: Not applicable.

Informed Consent Statement: Not applicable.

Data Availability Statement: Not applicable.

Conflicts of Interest: The authors declare no conflict of interest.

References

1. Wang, K.; Du, D.; Liu, G.; Chang, B.; Hong, Y. Microstructure and properties of WC reinforced Ni-based composite coatings with Y_2O_3 addition on titanium alloy by laser cladding. *Sci. Technol. Weld. Join.* **2019**, *24*, 517–524. [[CrossRef](#)]
2. Ke, J.; Liu, X.-B.; Liang, J.; Liang, L.; Luo, Y.-S. Microstructure and fretting wear of laser cladding self-lubricating anti-wear composite coatings on TA2 alloy after aging treatment. *Opt. Laser Technol.* **2019**, *119*, 105599. [[CrossRef](#)]
3. Chakraborty, S.S.; Dutta, S. Estimation of dilution in laser cladding based on energy balance approach using regression analysis. *Sādhanā* **2019**, *44*, 150. [[CrossRef](#)]
4. Nenadl, O.; Ocelík, V.; Palavra, A.; De Hosson, J.T. The Prediction of Coating Geometry from Main Processing Parameters in Laser Cladding. *Phys. Procedia* **2014**, *56*, 220–227. [[CrossRef](#)]
5. Wang, K.; Du, D.; Liu, G.; Chang, B.; Ju, J.; Sun, S.; Fu, H. Microstructure and property of laser clad Fe-based composite layer containing Nb and B4C powders. *J. Alloy. Compd.* **2019**, *802*, 373–384. [[CrossRef](#)]
6. Li, F.; Gao, Z.; Li, L.; Chen, Y. Microstructural study of MMC layers produced by combining wire and coaxial WC powder feeding in laser direct metal deposition. *Opt. Laser Technol.* **2016**, *77*, 134–143. [[CrossRef](#)]
7. Wang, K.; Du, D.; Liu, G.; Pu, Z.; Chang, B.; Ju, J. A study on the additive manufacturing of a high chromium Nickel-based superalloy by extreme high-speed laser metal deposition. *Opt. Laser Technol.* **2020**, *133*, 106504. [[CrossRef](#)]
8. Bhatnagar, S.; Mullick, S.; Gopinath, M. A lumped parametric analytical model for predicting molten pool temperature and clad geometry in pre-placed powder laser cladding. *Optik* **2021**, *247*, 168015. [[CrossRef](#)]
9. Frazier, W.E. Metal Additive Manufacturing: A Review. *J. Mater. Eng. Perform.* **2014**, *23*, 1917–1928. [[CrossRef](#)]
10. Syed, W.U.H.; Pinkerton, A.J.; Li, L. A comparative study of wire feeding and powder feeding in direct diode laser deposition for rapid prototyping. *Appl. Surf. Sci.* **2005**, *247*, 268–276. [[CrossRef](#)]
11. Dass, A.; Moridi, A. State of the Art in Directed Energy Deposition: From Additive Manufacturing to Materials Design. *Coatings* **2019**, *9*, 418. [[CrossRef](#)]
12. de Oliveira, U.; Ocelík, V.; De Hosson, J. Analysis of coaxial laser cladding processing conditions. *Surf. Coat. Technol.* **2005**, *197*, 127–136. [[CrossRef](#)]
13. Hao, M.; Sun, Y. A FEM model for simulating temperature field in coaxial laser cladding of Ti6Al4V alloy using an inverse modeling approach. *Int. J. Heat Mass Transf.* **2013**, *64*, 352–360. [[CrossRef](#)]
14. OuYang, C.-S.; Liu, X.-B.; Luo, Y.-S.; Liang, J.; Wang, M.; Chen, D.-Q. Preparation and high temperature tribological properties of laser in-situ synthesized self-lubricating composite coating on 304 stainless steel. *J. Mater. Res. Technol.* **2020**, *9*, 7034–7046. [[CrossRef](#)]
15. Xixi, L.; Kaikai, Z.; Jing, C.; Guanghui, M.; Fangli, Y.; Yingying, Z.; Hongwei, Z.; Peiqing, L.; Hui, X. Effect of line energy density of the laser beam on the microstructure and wear resistance properties of the obtained Fe3Al laser cladding coatings. *Optik* **2022**, *261*, 169256.
16. Ibrahim, M.Z.; Sarhan, A.A.; Yusuf, F.; Hamdi, M. Biomedical materials and techniques to improve the tribological, mechanical and biomedical properties of orthopedic implants—A review article. *J. Alloy. Compd.* **2017**, *714*, 636–667. [[CrossRef](#)]
17. Weng, F.; Chen, C.; Yu, H. Research status of laser cladding on titanium and its alloys: A review. *Mater. Des.* **2014**, *58*, 412–425. [[CrossRef](#)]
18. Chen, L.; Yu, T.; Xu, P.; Zhang, B. In-situ NbC reinforced Fe-based coating by laser cladding: Simulation and experiment. *Surf. Coat. Technol.* **2021**, *412*, 127027. [[CrossRef](#)]
19. Wang, W.; Wang, M.; Jie, Z.; Sun, F.; Huang, D. Research on the microstructure and wear resistance of titanium alloy structural members repaired by laser cladding. *Opt. Lasers Eng.* **2008**, *46*, 810–816. [[CrossRef](#)]
20. Sexton, L.; Lavin, S.; Byrne, G.; Kennedy, A. Laser cladding of aerospace materials. *J. Mater. Process. Technol.* **2002**, *122*, 63–68. [[CrossRef](#)]
21. Zeng, C.; Tian, W.; Liao, W.H.; Hua, L. Microstructure and porosity evaluation in laser-cladding deposited Ni-based coatings. *Surf. Coat. Technol.* **2016**, *294*, 122–130. [[CrossRef](#)]
22. Jin, G.; Cai, Z.; Guan, Y.; Cui, X.; Liu, Z.; Li, Y.; Dong, M.; Zhang, D. High temperature wear performance of laser-cladded FeNiCoAlCu high-entropy alloy coating. *Appl. Surf. Sci.* **2018**, *445*, 113–122. [[CrossRef](#)]
23. Liu, X.-B.; Meng, X.-J.; Liu, H.-Q.; Shi, G.-L.; Wu, S.-H.; Sun, C.-F.; Wang, M.-D.; Qi, L.-H. Development and characterization of laser clad high temperature self-lubricating wear resistant composite coatings on Ti-6Al-4V alloy. *Mater. Des.* **2014**, *55*, 404–409. [[CrossRef](#)]
24. Huang, C.; Zhang, Y.; Vilar, R.; Shen, J. Dry sliding wear behavior of laser clad TiVCrAlSi high entropy alloy coatings on Ti-6Al-4V substrate. *Mater. Des.* **2012**, *41*, 338–343. [[CrossRef](#)]
25. Abioye, T.; McCartney, D.; Clare, A. Laser cladding of Inconel 625 wire for corrosion protection. *J. Mater. Process. Technol.* **2015**, *217*, 232–240. [[CrossRef](#)]

26. Wang, G.; Liu, X.-B.; Zhu, G.-X.; Zhu, Y.; Liu, Y.-F.; Zhang, L.; Wang, J.-L. Tribological study of Ti₃SiC₂/Cu₅Si/TiC reinforced Co-based coatings on SUS304 steel by laser cladding. *Surf. Coat. Technol.* **2022**, *432*, 128064. [[CrossRef](#)]
27. El Cheikh, H.; Courant, B.; Branchu, S.; Hascoët, J.-Y.; Guillén, R. Analysis and prediction of single laser tracks geometrical characteristics in coaxial laser cladding process. *Opt. Lasers Eng.* **2012**, *50*, 413–422. [[CrossRef](#)]
28. Hamedi, M.; Torkamany, M.; Sabbaghzadeh, J. Effect of pulsed laser parameters on in-situ TiC synthesis in laser surface treatment. *Opt. Lasers Eng.* **2010**, *49*, 557–563. [[CrossRef](#)]
29. Ferreira, A.; Darabi, R.; Sousa, J.; Cruz, J.; Reis, A.; Vieira, M. Optimization of Direct Laser Deposition of a Martensitic Steel Powder (Metco 42C) on 42CrMo4 Steel. *Metals* **2021**, *11*, 672. [[CrossRef](#)]
30. Shan, B.; Chen, J.; Chen, S.; Ma, M.; Ni, L.; Shang, F.; Zhou, L. Laser cladding of Fe-based corrosion and wear-resistant alloy: Genetic design, microstructure, and properties. *Surf. Coat. Technol.* **2022**, *433*, 128117. [[CrossRef](#)]
31. Gan, Z.; Yu, G.; He, X.; Li, S. Numerical simulation of thermal behavior and multicomponent mass transfer in direct laser deposition of Co-base alloy on steel. *Int. J. Heat Mass Transf.* **2017**, *104*, 28–38. [[CrossRef](#)]
32. Janicki, D. Laser cladding of Inconel 625-based composite coatings reinforced by porous chromium carbide particles. *Opt. Laser Technol.* **2017**, *94*, 6–14. [[CrossRef](#)]
33. Fu, F.; Zhang, Y.; Chang, G.; Dai, J. Analysis on the physical mechanism of laser cladding crack and its influence factors. *Optik* **2016**, *127*, 200–202. [[CrossRef](#)]
34. Balu, P.; Leggett, P.; Hamid, S.; Kovacevic, R. Multi-Response Optimization of Laser-based Powder Deposition of Multi-track Single Layer Hastelloy C-276. *Mater. Manuf. Process.* **2013**, *28*, 173–182. [[CrossRef](#)]
35. Pant, P.; Chatterjee, D.; Nandi, T.; Samanta, S.K.; Lohar, A.K.; Changdar, A. Statistical modelling and optimization of clad characteristics in laser metal deposition of austenitic stainless steel. *J. Braz. Soc. Mech. Sci. Eng.* **2019**, *41*, 283. [[CrossRef](#)]
36. Devojno, O.G.; Feldshtein, E.; Kardapolava, M.A.; Lutsko, N.I. On the formation features, structure, microhardness and tribological behavior of single tracks and coating layers formed by laser cladding of Al-Fe powder bronze. *Surf. Coat. Technol.* **2019**, *358*, 195–206. [[CrossRef](#)]
37. Moeinfar, K.; Khodabakhshi, F.; Kashani-Bozorg, S.; Mohammadi, M.; Gerlich, A. A review on metallurgical aspects of laser additive manufacturing (LAM): Stainless steels, nickel superalloys, and titanium alloys. *J. Mater. Res. Technol.* **2022**, *16*, 1029–1068. [[CrossRef](#)]
38. Zhu, L.; Xue, P.; Lan, Q.; Meng, G.; Ren, Y.; Yang, Z.; Xu, P.; Liu, Z. Recent research and development status of laser cladding: A review. *Opt. Laser Technol.* **2021**, *138*, 106915. [[CrossRef](#)]
39. Zheng, Y.; Liu, F.; Gao, J.; Liu, F.; Huang, C.; Zheng, H.; Wang, P.; Qiu, H. Effect of different heat input on the microstructure and mechanical properties of laser cladding repaired 300M steel. *J. Mater. Res. Technol.* **2023**, *22*, 556–568. [[CrossRef](#)]
40. Ebrahimi, M.; Xie, Y.; Chi, C. Effect of cladding parameters on microstructure and defects in direct laser metal deposition of 24CrNiMo steel. *J. Laser Appl.* **2021**, *33*, 012007. [[CrossRef](#)]
41. Muvvala, G.; Karmakar, D.P.; Nath, A.K. Online monitoring of thermo-cycles and its correlation with microstructure in laser cladding of nickel based super alloy. *Opt. Lasers Eng.* **2017**, *88*, 139–152. [[CrossRef](#)]
42. Urbanic, R.J.; Saqib, S.M.; Aggarwal, K. Using Predictive Modeling and Classification Methods for Single and Overlapping Bead Laser Cladding to Understand Bead Geometry to Process Parameter Relationships. *J. Manuf. Sci. Eng.* **2016**, *138*, 051012. [[CrossRef](#)]
43. Goodarzi, D.M.; Pekkarinen, J.; Salminen, A. Analysis of laser cladding process parameter influence on the clad bead geometry. *Weld. World* **2017**, *61*, 883–891. [[CrossRef](#)]
44. Bax, B.; Rajput, R.; Kellet, R.; Reisacher, M. Systematic evaluation of process parameter maps for laser cladding and directed energy deposition. *Addit. Manuf.* **2018**, *21*, 487–494. [[CrossRef](#)]
45. Siddiqui, A.A.; Dubey, A.K. Recent trends in laser cladding and surface alloying. *Opt. Laser Technol.* **2020**, *134*, 106619. [[CrossRef](#)]
46. Cui, C.; Wu, M.; Miao, X.; Gong, Y.; Zhao, Z. The effect of laser energy density on the geometric characteristics, microstructure and corrosion resistance of Co-based coatings by laser cladding. *J. Mater. Res. Technol.* **2021**, *15*, 2405–2418. [[CrossRef](#)]
47. Yao, K.; Zongde, L.; Quanbing, L. Effect of Laser Power on Microstructure and Properties of Ni-based Alloy Coatings on 30CrMnSiA Steel. *J. Therm. Spray Technol.* **2022**, *31*, 2136–2146. [[CrossRef](#)]
48. Shamsaei, N.; Yadollahi, A.; Bian, L.; Thompson, S.M. An overview of Direct Laser Deposition for additive manufacturing; Part II: Mechanical behavior, process parameter optimization and control. *Addit. Manuf.* **2015**, *8*, 12–35. [[CrossRef](#)]
49. Zhao, Y.; Sun, J.; Guo, K.; Li, J. Investigation on the effect of laser remelting for laser cladding nickel based alloy. *J. Laser Appl.* **2019**, *31*, 022512. [[CrossRef](#)]
50. Pinkerton, A.J. Advances in the modeling of laser direct metal deposition. *J. Laser Appl.* **2015**, *27*, S15001. [[CrossRef](#)]
51. Bakhtiyari, A.N.; Wang, Z.; Wang, L.; Zheng, H. A review on applications of artificial intelligence in modeling and optimization of laser beam machining. *Opt. Laser Technol.* **2020**, *135*, 106721. [[CrossRef](#)]
52. Gao, J.; Wang, C.; Hao, Y.; Liang, X.; Zhao, K. Prediction of TC11 single-track geometry in laser metal deposition based on back propagation neural network and random forest. *J. Mech. Sci. Technol.* **2022**, *36*, 1417–1425. [[CrossRef](#)]
53. Yu, D.; Wang, C.; Cheng, X.; Zhang, F. Optimization of hybrid PVD process of TiAlN coatings by Taguchi method. *Appl. Surf. Sci.* **2008**, *255*, 1865–1869. [[CrossRef](#)]
54. Mahamood, R.; Akinlabi, E.; Shukla, M.; Pityana, S. Scanning velocity influence on microstructure, microhardness and wear resistance performance of laser deposited Ti₆Al₄V/TiC composite. *Mater. Des.* **2013**, *50*, 656–666. [[CrossRef](#)]

55. Liu, J.; Li, J.; Cheng, X.; Wang, H. Effect of dilution and macrosegregation on corrosion resistance of laser clad AerMet100 steel coating on 300M steel substrate. *Surf. Coat. Technol.* **2017**, *325*, 352–359. [[CrossRef](#)]
56. Weng, F.; Yu, H.; Chen, C.; Liu, J.; Zhao, L.; Dai, J.; Zhao, Z. Effect of process parameters on the microstructure evolution and wear property of the laser cladding coatings on Ti-6Al-4V alloy. *J. Alloy. Compd.* **2016**, *692*, 989–996. [[CrossRef](#)]
57. Yi, P.; Zhan, X.; He, Q.; Liu, Y.; Xu, P.; Xiao, P.; Jia, D. Influence of laser parameters on graphite morphology in the bonding zone and process optimization in gray cast iron laser cladding. *Opt. Laser Technol.* **2018**, *109*, 480–487. [[CrossRef](#)]
58. Gu, J.; Ju, J.; Wang, R.; Li, J.; Yu, H.; Wang, K. Effects of Laser Scanning Rate and Ti Content on Wear of Novel Fe-Cr-B-Al-Ti Coating Prepared via Laser Cladding. *J. Therm. Spray Technol.* **2022**, *31*, 2609–2620. [[CrossRef](#)]
59. Srisungsitthisunti, P.; Kaewprachum, B.; Yang, Z.; Gao, G. Real-Time Quality Monitoring of Laser Cladding Process on Rail Steel by an Infrared Camera. *Metals* **2022**, *12*, 825. [[CrossRef](#)]
60. Zhang, H.; Pan, Y.; Zhang, Y.; Lian, G.; Cao, Q.; Yang, J. Influence of laser power on the microstructure and properties of in-situ NbC/WCoB-TiC coating by laser cladding. *Mater. Chem. Phys.* **2022**, *290*, 126636. [[CrossRef](#)]
61. Li, M.; Huang, J.; Zhu, Y.Y.; Li, Z.G.; Wu, Y.X. Effect of laser scanning speed on TiN/TiB-Ti based composite. *Surf. Eng.* **2013**, *29*, 346–350. [[CrossRef](#)]
62. Jiao, X.; Wang, J.; Wang, C.; Gong, Z.; Pang, X.; Xiong, S. Effect of laser scanning speed on microstructure and wear properties of T15M cladding coating fabricated by laser cladding technology. *Opt. Lasers Eng.* **2018**, *110*, 163–171. [[CrossRef](#)]
63. Bartkowski, D.; Kinal, G. Microstructure and wear resistance of Stellite-6/WC MMC coatings produced by laser cladding using Yb:YAG disk laser. *Int. J. Refract. Met. Hard Mater.* **2016**, *58*, 157–164. [[CrossRef](#)]
64. Chao, Q.; Guo, T.; Jarvis, T.; Wu, X.; Hodgson, P.; Fabijanic, D. Direct laser deposition cladding of Al CoCrFeNi high entropy alloys on a high-temperature stainless steel. *Surf. Coat. Technol.* **2017**, *332*, 440–451. [[CrossRef](#)]
65. Chryssoulouris, G.; Zannis, S.; Tsirbas, K.; Lalas, C. An Experimental Investigation of Laser Cladding. *CIRP Ann.* **2002**, *51*, 145–148. [[CrossRef](#)]
66. Qu, C.; Li, J.; Bai, L.; Shao, J.; Song, R.; Chen, J. Effects of the thickness of the pre-placed layer on microstructural evolution and mechanical properties of the laser-clad coatings. *J. Alloy. Compd.* **2015**, *644*, 450–463. [[CrossRef](#)]
67. Fu, Y.; Downey, A.R.; Yuan, L.; Zhang, T.; Pratt, A.; Balogun, Y. Machine learning algorithms for defect detection in metal laser-based additive manufacturing: A review. *J. Manuf. Process.* **2022**, *75*, 693–710. [[CrossRef](#)]
68. Davim, J.P.; Oliveira, C.; Cardoso, A. Predicting the geometric form of clad in laser cladding by powder using multiple regression analysis (MRA). *Mater. Des.* **2008**, *29*, 554–557. [[CrossRef](#)]
69. Huang, Y.; Yuan, S. Modeling the geometric formation and powder deposition mass in laser induction hybrid cladding. *J. Mech. Sci. Technol.* **2012**, *26*, 2347–2351. [[CrossRef](#)]
70. Shi, J.; Zhu, P.; Fu, G.; Shi, S. Geometry characteristics modeling and process optimization in coaxial laser inside wire cladding. *Opt. Laser Technol.* **2018**, *101*, 341–348. [[CrossRef](#)]
71. Ansari, M.; Razavi, R.S.; Barekat, M. An empirical-statistical model for coaxial laser cladding of NiCrAlY powder on Inconel 738 superalloy. *Opt. Laser Technol.* **2016**, *86*, 136–144. [[CrossRef](#)]
72. Shayanfar, P.; Daneshmanesh, H.; Janghorban, K. Parameters Optimization for Laser Cladding of Inconel 625 on ASTM A592 Steel. *J. Mater. Res. Technol.* **2020**, *9*, 8258–8265. [[CrossRef](#)]
73. Erfanmanesh, M.; Abdollah-Pour, H.; Mohammadian-Semnani, H.; Shoja-Razavi, R. An empirical-statistical model for laser cladding of WC-12Co powder on AISI 321 stainless steel. *Opt. Laser Technol.* **2017**, *97*, 180–186. [[CrossRef](#)]
74. Nabhani, M.; Razavi, R.S.; Barekat, M. An empirical-statistical model for laser cladding of Ti-6Al-4V powder on Ti-6Al-4V substrate. *Opt. Laser Technol.* **2018**, *100*, 265–271. [[CrossRef](#)]
75. Javid, Y. Multi-response optimization in laser cladding process of WC powder on Inconel 718. *CIRP J. Manuf. Sci. Technol.* **2020**, *31*, 406–417. [[CrossRef](#)]
76. Huang, Y.; Hu, Y.; Zhang, M.; Mao, C.; Wang, K.; Tong, Y.; Zhang, J.; Li, K. Multi-Objective Optimization of Process Parameters in Laser Cladding CoCrCuFeNi High-Entropy Alloy Coating. *J. Therm. Spray Technol.* **2022**, *31*, 1985–2000. [[CrossRef](#)]
77. Bose, S.; Nandi, T. Microstructural characterization and measurement of laser responses of lens developed novel titanium matrix composite. *Eur. Phys. J. Plus* **2021**, *136*, 978. [[CrossRef](#)]
78. Badkar, D.S.; Pandey, K.S.; Buvanashakaran, G. Application of the central composite design in optimization of laser transformation hardening parameters of commercially pure titanium using Nd:YAG laser. *Int. J. Adv. Manuf. Technol.* **2011**, *59*, 169–192. [[CrossRef](#)]
79. Sun, Y.; Hao, M. Statistical analysis and optimization of process parameters in Ti6Al4V laser cladding using Nd:YAG laser. *Opt. Lasers Eng.* **2012**, *50*, 985–995. [[CrossRef](#)]
80. Dada, M.; Popoola, P.; Mathe, N.; Pityana, S.; Adeosun, S. Parametric optimization of laser deposited high entropy alloys using response surface methodology (RSM). *Int. J. Adv. Manuf. Technol.* **2020**, *109*, 2719–2732. [[CrossRef](#)]
81. Guo, C.; He, S.; Yue, H.; Li, Q.; Hao, G. Prediction modelling and process optimization for forming multi-layer cladding structures with laser directed energy deposition. *Opt. Laser Technol.* **2020**, *134*, 106607. [[CrossRef](#)]
82. Cui, L.-J.; Zhang, M.; Guo, S.-R.; Cao, Y.-L.; Zeng, W.-H.; Li, X.-L.; Zheng, B. Multi-objective numerical simulation of geometrical characteristics of laser cladding of cobalt-based alloy based on response surface methodology. *Meas. Control.* **2020**, *54*, 1125–1135. [[CrossRef](#)]
83. Li, T.; Long, H.; Qiu, C.; Wang, M.; Li, D.; Dong, Z.; Gui, Y. Multi-Objective Optimization of Process Parameters of 45 Steel Laser Cladding Ni60PTA Alloy Powder. *Coatings* **2022**, *12*, 939. [[CrossRef](#)]

84. Wu, Z.; Li, T.; Li, Q.; Shi, B.; Li, X.; Wang, X.; Lu, H.; Zhang, H.-C. Process optimization of laser cladding Ni60A alloy coating in remanufacturing. *Opt. Laser Technol.* **2019**, *120*, 105718. [[CrossRef](#)]
85. Khorram, A.; Jamaloei, A.D.; Paidar, M.; Cao, X. Laser cladding of Inconel 718 with 75Cr3C2 + 25(80Ni20Cr) powder: Statistical modeling and optimization. *Surf. Coat. Technol.* **2019**, *378*, 124933. [[CrossRef](#)]
86. Lian, G.; Yao, M.; Zhang, Y.; Chen, C. Analysis and prediction on geometric characteristics of multi-track overlapping laser cladding. *Int. J. Adv. Manuf. Technol.* **2018**, *97*, 2397–2407. [[CrossRef](#)]
87. Wu, S.; Liu, Z.; Huang, X.; Wu, Y.; Gong, Y. Process parameter optimization and EBSD analysis of Ni60A-25% WC laser cladding. *Int. J. Refract. Met. Hard Mater.* **2021**, *101*, 105675. [[CrossRef](#)]
88. Ben-Arfa, B.A.; Salvado, I.M.M.; Frade, J.R.; Pullar, R.C. Fast route for synthesis of stoichiometric hydroxyapatite by employing the Taguchi method. *Mater. Des.* **2016**, *109*, 547–555. [[CrossRef](#)]
89. Liu, Y.; Liu, C.; Liu, W.; Ma, Y.; Tang, S.; Liang, C.; Cai, Q.; Zhang, C. Optimization of parameters in laser powder deposition AlSi10Mg alloy using Taguchi method. *Opt. Laser Technol.* **2018**, *111*, 470–480. [[CrossRef](#)]
90. Lin, C.-M. Parameter optimization of laser cladding process and resulting microstructure for the repair of tenon on steam turbine blade. *Vacuum* **2015**, *115*, 117–123. [[CrossRef](#)]
91. Xu, M.; Li, J.; Jiang, J.; Li, B. Influence of Powders and Process Parameters on Bonding Shear Strength and Micro Hardness in Laser Cladding Remanufacturing. *Procedia CIRP* **2015**, *29*, 804–809. [[CrossRef](#)]
92. Quazi, M.M.; Fazal, M.A.; Haseeb, A.S.M.A.; Yusof, F.; Masjuki, H.H.; Arslan, A. Laser Composite Surfacing of Ni-WC Coating on AA5083 for Enhancing Tribomechanical Properties. *Tribol. Trans.* **2016**, *60*, 249–259. [[CrossRef](#)]
93. Chen, L.; Yu, T.; Chen, X.; Zhao, Y.; Guan, C. Process optimization, microstructure and microhardness of coaxial laser cladding TiC reinforced Ni-based composite coatings. *Opt. Laser Technol.* **2022**, *152*, 108129. [[CrossRef](#)]
94. Shi, Y.; Li, Y.; Liu, J.; Yuan, Z. Investigation on the parameter optimization and performance of laser cladding a gradient composite coating by a mixed powder of Co50 and Ni/WC on 20CrMnTi low carbon alloy steel. *Opt. Laser Technol.* **2018**, *99*, 256–270. [[CrossRef](#)]
95. Zhang, Z.; Kovacevic, R. Multiresponse Optimization of Laser Cladding Steel + VC Using Grey Relational Analysis in the Taguchi Method. *JOM* **2016**, *68*, 1762–1773. [[CrossRef](#)]
96. Mondal, S.; Paul, C.P.; Kukreja, L.M.; Bandyopadhyay, A.; Pal, P.K. Application of Taguchi-based gray relational analysis for evaluating the optimal laser cladding parameters for AISI1040 steel plane surface. *Int. J. Adv. Manuf. Technol.* **2012**, *66*, 91–96. [[CrossRef](#)]
97. Deng, D.; Li, T.; Huang, Z.; Jiang, H.; Yang, S.; Zhang, Y. Multi-response optimization of laser cladding for TiC particle reinforced Fe matrix composite based on Taguchi method and grey relational analysis. *Opt. Laser Technol.* **2022**, *153*, 108259. [[CrossRef](#)]
98. Yu, T.; Yang, L.; Zhao, Y.; Sun, J.; Li, B. Experimental research and multi-response multi-parameter optimization of laser cladding Fe313. *Opt. Laser Technol.* **2018**, *108*, 321–332. [[CrossRef](#)]
99. Fan, P.; Zhang, G. Study on process optimization of WC-Co50 cermet composite coating by laser cladding. *Int. J. Refract. Met. Hard Mater.* **2019**, *87*, 105133. [[CrossRef](#)]
100. Marzbanrad, J.; Ghaseminejad, P.; Ahmadzadeh, M.H.; Teimouri, R. Experimental investigation and statistical optimization of laser surface cladding parameters. *Int. J. Adv. Manuf. Technol.* **2014**, *76*, 1163–1172. [[CrossRef](#)]
101. Wang, Q.; Zeng, X.; Chen, C.; Lian, G.; Huang, X. An Integrated Method for Multi-Objective Optimization of Multi-Pass Fe50/TiC Laser Cladding on AISI 1045 Steel based on Grey Relational Analysis and Principal Component Analysis. *Coatings* **2020**, *10*, 151. [[CrossRef](#)]
102. Liang, W.; Yang, Y.; Qi, K.; Jin, K.; Xiong, L. Quality evaluation of multi-path laser cladding coatings based on integrated fuzzy comprehensive evaluation and improved analytical hierarchy process method. *Surf. Coat. Technol.* **2021**, *427*, 127816. [[CrossRef](#)]
103. Reddy, L.; Preston, S.; Shipway, P.; Davis, C.; Hussain, T. Process parameter optimisation of laser clad iron based alloy: Predictive models of deposition efficiency, porosity and dilution. *Surf. Coat. Technol.* **2018**, *349*, 198–207. [[CrossRef](#)]
104. Meng, G.; Zhu, L.; Zhang, J.; Yang, Z.; Xue, P. Statistical analysis and multi-objective process optimization of laser cladding TiC-Inconel718 composite coating. *Optik* **2021**, *240*, 166828. [[CrossRef](#)]
105. Menghani, J.; Vyas, A.; More, S.; Paul, C.; Patnaik, A. Parametric investigation and optimization for CO₂ laser cladding of AlFeCoCrNiCu powder on AISI 316. *High Temp. Mater. Process.* **2021**, *40*, 265–280. [[CrossRef](#)]
106. Mohammed, S.; Zhang, Z.; Kovacevic, R. Optimization of processing parameters in fiber laser cladding. *Int. J. Adv. Manuf. Technol.* **2020**, *111*, 2553–2568. [[CrossRef](#)]
107. Liu, S.; Kovacevic, R. Statistical analysis and optimization of processing parameters in high-power direct diode laser cladding. *Int. J. Adv. Manuf. Technol.* **2014**, *74*, 867–878. [[CrossRef](#)]
108. Mahamood, R.M.; Akinlabi, E.T. Processing Parameters Optimization for Material Deposition Efficiency in Laser Metal Deposited Titanium Alloy. *Lasers Manuf. Mater. Process.* **2015**, *3*, 9–21. [[CrossRef](#)]
109. Moradi, M.; Hasani, A.; Pourmand, Z.; Lawrence, J. Direct laser metal deposition additive manufacturing of Inconel 718 superalloy: Statistical modelling and optimization by design of experiments. *Opt. Laser Technol.* **2021**, *144*, 107380. [[CrossRef](#)]
110. Akbari, M.; Saedodin, S.; Panjehpour, A.; Hassani, M.; Afrand, M.; Torkamany, M.J. Numerical simulation and designing artificial neural network for estimating melt pool geometry and temperature distribution in laser welding of Ti6Al4V alloy. *Optik* **2016**, *127*, 11161–11172. [[CrossRef](#)]

111. Shakeri, S.; Ghassemi, A.; Hassani, M.; Hajian, A. Investigation of material removal rate and surface roughness in wire electrical discharge machining process for cementation alloy steel using artificial neural network. *Int. J. Adv. Manuf. Technol.* **2015**, *82*, 549–557. [[CrossRef](#)]
112. Yin, F.; Mao, H.; Hua, L. A hybrid of back propagation neural network and genetic algorithm for optimization of injection molding process parameters. *Mater. Des.* **2011**, *32*, 3457–3464. [[CrossRef](#)]
113. Mohajernia, B.; Mirazimzadeh, S.E.; Pasha, A.; Urbanic, R.J. Machine learning approaches for predicting geometric and mechanical characteristics for single P420 laser beads clad onto an AISI 1018 substrate. *Int. J. Adv. Manuf. Technol.* **2021**, *118*, 3691–3710. [[CrossRef](#)]
114. Mondal, S.; Bandyopadhyay, A.; Pal, P.K. Application of artificial neural network for the prediction of laser cladding process characteristics at Taguchi-based optimized condition. *Int. J. Adv. Manuf. Technol.* **2013**, *70*, 2151–2158. [[CrossRef](#)]
115. Aggarwal, K.; Urbanic, R.J.; Saqib, S.M. Development of predictive models for effective process parameter selection for single and overlapping laser clad bead geometry. *Rapid Prototyp. J.* **2018**, *24*, 214–228. [[CrossRef](#)]
116. Hongyu, L.; Hui, C.; Ying, W.; Yong, C.; Wei, Y. Prediction of two-dimensional topography of laser cladding based on neural network. *Int. J. Mod. Phys. B* **2019**, *33*, 1940034. [[CrossRef](#)]
117. Song, C.; Liu, L.; Yang, Y.; Weng, C. Prediction on Geometrical Characteristics of Laser Energy Deposition Based on Regression Equation and Neural Network. *IFAC-PapersOnLine* **2020**, *53*, 89–96. [[CrossRef](#)]
118. Li, Y.; Wang, K.; Fu, H.; Zhi, X.; Guo, X.; Lin, J. Prediction for Dilution Rate of AlCoCrFeNi Coatings by Laser Cladding Based on a BP Neural Network. *Coatings* **2021**, *11*, 1402. [[CrossRef](#)]
119. Caiazzo, F.; Caggiano, A. Laser Direct Metal Deposition of 2024 Al Alloy: Trace Geometry Prediction via Machine Learning. *Materials* **2018**, *11*, 444. [[CrossRef](#)]
120. Guo, S.; Chen, Z.; Cai, D.; Zhang, Q.; Kovalenko, V.; Yao, J. Prediction of Simulating and Experiments for Co-based Alloy Laser Cladding by HPDL. *Phys. Procedia* **2013**, *50*, 375–382. [[CrossRef](#)]
121. Kumar, A.; Maji, K. Selection of Process Parameters for Near-Net Shape Deposition in Wire Arc Additive Manufacturing by Genetic Algorithm. *J. Mater. Eng. Perform.* **2020**, *29*, 3334–3352. [[CrossRef](#)]
122. Yang, S.; Bai, H.; Li, C.; Shu, L.; Zhang, X.; Jia, Z. Numerical Simulation and Multi-Objective Parameter Optimization of Inconel718 Coating Laser Cladding. *Coatings* **2022**, *12*, 708. [[CrossRef](#)]
123. Ahsan, N.; Khoda, B. AM optimization framework for part and process attributes through geometric analysis. *Addit. Manuf.* **2016**, *11*, 85–96. [[CrossRef](#)]
124. Liu, J.C.; Ni, L.B. Prediction of laser clad parameters based on neural network. *Mater. Technol.* **2012**, *27*, 11–14. [[CrossRef](#)]
125. Xu, Z.M.; Wu, H.B.; Hong, Z.H. Quality Prediction of Laser Cladding Based on Evolutionary Neural Network. *Appl. Mech. Mater.* **2010**, *44–47*, 1012–1017. [[CrossRef](#)]
126. Liu, H.; Qin, X.; Huang, S.; Jin, L.; Wang, Y.; Lei, K. Geometry Characteristics Prediction of Single Track Cladding Deposited by High Power Diode Laser Based on Genetic Algorithm and Neural Network. *Int. J. Precis. Eng. Manuf.* **2018**, *19*, 1061–1070. [[CrossRef](#)]
127. Pang, Y.; Fu, G.; Wang, M.; Gong, Y.; Yu, S.; Xu, J.; Liu, F. Parameter Optimization of High Deposition Rate Laser Cladding Based on the Response Surface Method and Genetic Neural Network Model. *Chin. J. Lasers* **2021**, *48*, 0602112. [[CrossRef](#)]
128. Yu, J.; Sun, W.; Huang, H.; Wang, W.; Hu, Y. Crack Sensitivity Control of Nickel-Based Laser Coating Based on Genetic Algorithm and Neural Network. *Coatings* **2019**, *9*, 728. [[CrossRef](#)]
129. Youwen, Y.; Zongjun, T.; Hu, P.; Dongsheng, W.; Lida, S. Geometry quality prediction of Ni-based superalloy coating by laser cladding based on neural network and genetic algorithm. *Trans. China Weld. Inst.* **2013**, *34*, 78–82.
130. Xiao, T.T.; Cai, C.Z.; Tang, J.L.; Huang, S.J. Modeling of transition temperature for pulsed laser deposition NdBa2Cu3O7- δ thin films via support vector regression. *Int. J. Mod. Phys. B* **2013**, *27*, 1362040. [[CrossRef](#)]
131. Pan, X.; Pang, X.; Wang, H.; Xu, Y. A safe screening based framework for support vector regression. *Neurocomputing* **2018**, *287*, 163–172. [[CrossRef](#)]
132. Wang, T.; Qi, J.; Xu, H.; Wang, Y.; Liu, L.; Gao, D. Fault diagnosis method based on FFT-RPCA-SVM for Cascaded-Multilevel Inverter. *ISA Trans.* **2016**, *60*, 156–163. [[CrossRef](#)] [[PubMed](#)]
133. He, Z.; Zeng, Y.; Shao, H.; Hu, H.; Xu, X. Novel motor fault detection scheme based on one-class tensor hyperdisk. *Knowl. Based Syst.* **2023**, *262*, 110259. [[CrossRef](#)]
134. Chen, T.; Wu, W.; Li, W.; Liu, D. Laser cladding of nanoparticle TiC ceramic powder: Effects of process parameters on the quality characteristics of the coatings and its prediction model. *Opt. Laser Technol.* **2019**, *116*, 345–355. [[CrossRef](#)]
135. Chen, X.; Xiao, M.; Kang, D.; Sang, Y.; Zhang, Z.; Jin, X. Prediction of Geometric Characteristics of Melt Track Based on Direct Laser Deposition Using M-SVR Algorithm. *Materials* **2021**, *14*, 7221. [[CrossRef](#)] [[PubMed](#)]
136. Yao, W.; Huang, Y.; Yang, Y. Size Prediction of Directed Energy Deposited Cladding Tracks Based on Support Vector Regression. *Chin. J. Lasers* **2020**, *47*, 0802007. [[CrossRef](#)]
137. Zhang, Y.; Gong, B.; Tang, Z.; Cao, W. Application of a Bio-Inspired Algorithm in the Process Parameter Optimization of Laser Cladding. *Machines* **2022**, *10*, 263. [[CrossRef](#)]
138. Jaber, A.; Lafon, P.; Younes, R. A branch-and-bound algorithm based on NSGAI1 for multi-objective mixed integer nonlinear optimization problems. *Eng. Optim.* **2021**, *54*, 1004–1022. [[CrossRef](#)]

139. Peng, S.; Li, T.; Zhao, J.; Lv, S.; Tan, G.Z.; Dong, M.; Zhang, H. Towards energy and material efficient laser cladding process: Modeling and optimization using a hybrid TS-GEP algorithm and the NSGA-II. *J. Clean. Prod.* **2019**, *227*, 58–69. [[CrossRef](#)]
140. Jiang, X.; Tian, Z.; Liu, W.; Tian, G.; Gao, Y.; Xing, F.; Suo, Y.; Song, B. An energy-efficient method of laser remanufacturing process. *Sustain. Energy Technol. Assess.* **2022**, *52*, 102201. [[CrossRef](#)]
141. Shu, L.; Li, J.; Wu, H.; Heng, Z. Optimization of Multi-Track Laser-Cladding Process of Titanium Alloy Based on RSM and NSGA-II Algorithm. *Coatings* **2022**, *12*, 1301. [[CrossRef](#)]
142. Zhao, K.; Liang, X.; Wang, W.; Yang, P.; Hao, Y.; Zhu, Z. Multi-Objective Optimization of Coaxial Powder Feeding Laser Cladding Based on NSGA-II. *Chin. J. Lasers* **2020**, *47*, 0102004. [[CrossRef](#)]
143. Vahabli, E.; Rahmati, S. Improvement of FDM parts' surface quality using optimized neural networks—medical case studies. *Rapid Prototyp. J.* **2017**, *23*, 825–842. [[CrossRef](#)]
144. Adedeji, P.A.; Akinlabi, S.A.; Madushele, N.; Olatunji, O.O. Hybrid neurofuzzy wind power forecast and wind turbine location for embedded generation. *Int. J. Energy Res.* **2020**, *45*, 413–428. [[CrossRef](#)]
145. Xu, S.-H.; Mu, X.-D.; Chai, D.; Zhao, P. Multi-objective quantum-behaved particle swarm optimization algorithm with double-potential well and share-learning. *Optik* **2016**, *127*, 4921–4927. [[CrossRef](#)]
146. Pant, P.; Chatterjee, D. Prediction of clad characteristics using ANN and combined PSO-ANN algorithms in laser metal deposition process. *Surf. Interfaces* **2020**, *21*, 100699. [[CrossRef](#)]
147. Deng, Z.; Chen, T.; Wang, H.; Li, S.; Liu, D. Process Parameter Optimization When Preparing Ti(C, N) Ceramic Coatings Using Laser Cladding Based on a Neural Network and Quantum-Behaved Particle Swarm Optimization Algorithm. *Appl. Sci.* **2020**, *10*, 6331. [[CrossRef](#)]
148. Ma, M.; Xiong, W.; Lian, Y.; Han, D.; Zhao, C.; Zhang, J. Modeling and optimization for laser cladding via multi-objective quantum-behaved particle swarm optimization algorithm. *Surf. Coat. Technol.* **2019**, *381*, 125129. [[CrossRef](#)]
149. Ngwoke, C.C.; Mahamood, R.M.; Aigbodion, V.S.; Jen, T.-C.; Adedeji, P.A.; Akinlabi, E.T. Soft computing-based process optimization in laser metal deposition of Ti-6Al-4 V. *Int. J. Adv. Manuf. Technol.* **2022**, *120*, 1079–1093. [[CrossRef](#)]
150. Singh, A.K.; Bal, K.S.; Dey, D.; Das, A.K.; Pal, A.R.; Pratihar, D.K.; Choudhury, A.R. Experimental investigation and parametric optimization for minimization of dilution during direct laser metal deposition of tungsten carbide and cobalt powder mixture on SS304 substrate. *Powder Technol.* **2021**, *390*, 339–353. [[CrossRef](#)]
151. Zhou, Z.; Du, Y.; He, G.; Xu, L.; Shu, L. Optimization and Characterization of Laser Cladding of 15-5PH Coating on 20Cr13 Stainless Steel. *J. Mater. Eng. Perform.* **2022**, *32*, 962–977. [[CrossRef](#)]
152. Sohrabpoor, H. Analysis of laser powder deposition parameters: ANFIS modeling and ICA optimization. *Optik* **2016**, *127*, 4031–4038. [[CrossRef](#)]
153. Liang, X.; Wang, W.; Zhao, K.; Hao, Y.; Yang, P.; Zhu, Z. Application of random forest re-gression analysis in trace geometry prediction of laser cladding. *Chin. J. Nonferrous Met.* **2020**, *30*, 1644–1652. [[CrossRef](#)]

Disclaimer/Publisher's Note: The statements, opinions and data contained in all publications are solely those of the individual author(s) and contributor(s) and not of MDPI and/or the editor(s). MDPI and/or the editor(s) disclaim responsibility for any injury to people or property resulting from any ideas, methods, instructions or products referred to in the content.